Earth-Science Reviews 110 (2012) 1–25

Contents lists available at SciVerse ScienceDirect

Earth-Science Reviews

journal homepage: www.elsevier.com/locate/earscirev

Dynamics and evolution of the deep mantle resulting from thermal, chemical, phase and melting effects

Paul J. Tackley *

Institute of Geophysics, Department of Earth Sciences, ETH Zürich, Sonneggstrasse 5, 8092 Zurich, Switzerland

ARTICLE INFO

Article history:
Received 22 June 2011
Accepted 3 October 2011
Available online 10 October 2011

Keywords:
Mantle convection
Core–mantle boundary
D″
Post-perovskite
Ultra-low velocity zone

ABSTRACT

The core–mantle boundary (CMB) – the interface between the silicate mantle and liquid iron alloy outer core – is the most important boundary inside our planet, with processes occurring in the deep mantle above it playing a major role in the evolution of both the core and the mantle. The last decade has seen an astonishing improvement in our knowledge of this region due to improvements in seismological data and techniques for mapping both large- and small-scale structures, mineral physics discoveries such as post-perovskite and the iron spin transition, and dynamical modelling. The deep mantle is increasingly revealed as a very complex region characterised by large variations in temperature and composition, phase changes, melting (possibly at present and certainly in the past), and anisotropic structures. Here, some fundamentals of the relevant processes and uncertainties are reviewed in the context of long-term Earth evolution and how it has led to the observed present-day structures. Melting has been a dominant process in Earth's evolution. Several processes involving melting, some of which operated soon after Earth's formation and some of which operated throughout its history, have produced dense, iron rich material that has likely sunk to the deepest mantle to be incorporated into a heterogeneous basal mélange (BAM) that is now evident seismically as two large low-velocity regions under African and the Pacific, but was probably much larger in the past. This BAM modulates core heat flux, plume formation and the separation of different slab components, and may contain various trace-element cocktails required to explain geochemical observations. The geographical location of BAM material has, however, probably changed through Earth's history due to the inherent time-dependence of plate tectonics and continental cycles.

Contents

* Tel.: +41 446332758; fax: +41 446331065.
E-mail address: ptackley@ethz.ch.

0012-8252/$ – see front matter © 2011 Elsevier B.V. All rights reserved.
doi:10.1016/j.earscirev.2011.10.001

1. Introduction

The core–mantle boundary (CMB) is the interface between the solid rocky silicate mantle and liquid iron alloy outer core. This interface has a large density contrast and is the most important boundary inside our planet. As seismologists probe the CMB region with ever improving techniques and data, it is increasingly found to be a very complex region containing large variations in temperature and composition, phase changes, melting (possibly at present and certainly in the past), and anisotropic structures. The complexity in this deep mantle region above the CMB is second only to that in the Earth's near-surface region (i.e. the crust and lithosphere). Processes occurring above the CMB influence the evolution of both the core and the mantle.

Large temperature variations arise because the deep mantle contains the lower thermal boundary layer of the convecting mantle, with the temperature rise from an average mantle adiabat to the top of the core being in the range 1200–1800 K: here, cold downwelling slabs pool and heat up, and hot upwelling plumes can form. Compositional variations are not surprising due to the large density jump between silicate rock and metal, which makes the region above the CMB a natural accumulation zone for rock that is denser than average mantle and therefore sinks, but is less dense than the core — just as the region below Earth's surface (the crust) is an accumulation zone for rock that is less dense than the mantle below. Our knowledge of deep mantle phase changes has undergone a near-revolution in the last 8 years, in particular with the discovery of a transition from perovskite, the dominant lower mantle mineral, to post-perovskite; much mineral physics research has been devoted to determining the details of this transition. Additionally, it was discovered that the electronic spin state of iron in mantle minerals undergoes a transition with increasing pressure, which could influence the physical properties from mid-mantle to CMB pressures depending on composition and temperature.

The goal of this review is to summarise the fundamental physics of relevant processes in the context of long-term Earth evolution, and examine how they may have led to what is observed in the present-day Earth. The next section covers dynamics arising from thermal buoyancy, then there is a section on the interaction of compositional and thermal buoyancy (thermo-chemical convection), and then sections focussing on the influence of the post-perovskite transition and the causes and dynamical implications of ultra-low velocity zones (ULVZs). Finally, there is a discussion and synthesis.

2. Thermal convection

2.1. Background

Mantle convection and plate tectonics are an integrated system, and are the engine that drives the dynamic solid Earth, causing continental drift, mountain building, allowing the Earth to lose the heat that it gets from radiogenic heating and from its formation, and controlling heat loss from the core, which drives the geodynamo. The deepest mantle, directly above the CMB, is the lower thermal boundary layer (TBL) of this convecting system, and has a large temperature drop across it.

The temperature drop across this lower TBL can be estimated by subtracting the temperature of an average mantle adiabat extrapolated to ~2700 km depth (because the interior of a convecting system adopts an approximately adiabatic profile), from the estimated CMB temperature. For the former, the mantle potential temperature is typically estimated to be ~1600 K based on the petrology of basalts (e.g. Herzberg et al. (2007); McKenzie and Bickle (1988)), which when extrapolated to ~2700 km depth gives temperature estimates in the range 2400–2700 K (e.g. Brown and Shankland (1981); Katsura et al. (2010)). The CMB temperature is more difficult to constrain. Estimates of the CMB temperature come from consideration of the core phase diagram: the outer core is above the liquidus, and the temperature at the inner core boundary (ICB) adiabatically extrapolated to the CMB gives the CMB temperature. The ICB temperature is, unfortunately, still uncertain by approximately 2000 K (Dubrovinsky and Lin, 2009) because of uncertainties in the core composition and in the measured or calculated values. Nevertheless, estimates of CMB temperature have been made, notably 3700–4300 K (Boehler, 2000) and 3950–4200 K (Price et al., 2004), both consistent with the lower bound of 3300 K based on melting of Fe–Si alloy (Asanuma et al., 2010). Another estimate of CMB temperature comes from combining seismological observations of deep mantle structures with high-P,T elastic properties of minerals, leading to a CMB temperature of 3800 ± 200 K (Kawai and Tsuchiya, 2009). A CMB temperature of ~4000 K thus satisfies all constraints. Combining the estimates of CMB temperature with the estimates of deep mantle adiabat leads to a temperature drop in the range ~1200–1800 K.

The deep mantle has often been thought of as a 'slab graveyard' where subducted slabs, sinking because they are cold, pool and are warmed by heat from the core. Evidence for this is that seismic tomographic images convincingly show slabs penetrating the 660 km discontinuity, sometimes after temporarily stagnating at the base of the transition zone (Fukao, 1992; Van der Hilst et al., 1997; Grand, 2002; Zhao, 2009) and that seismically fast regions above the CMB correlate well with historical subduction zones (Richards and Engebretson, 1992; Ricard et al., 1993; Kyvalova et al., 1995; Van der Voo et al., 1999a,b; Becker and Boschi, 2002; van der Meer et al., 2010).

The upwelling part of mantle convection is a combination of two components: a distributed return flow characteristic of convection in a system with much internal heating (e.g. Bercovici et al., 1989; Glatzmaier et al., 1990; Houseman, 1988; Schubert and Zebib, 1980), and focussed cylindrical plumes, which are thought to provide a

good explanation for some, although not all, of the 'hotspots' observed at Earth's surface (e.g. Morgan, 1971; Richards et al., 1989; Steinberger, 2000).

The locations of plumes at the CMB, as well as time-variations in the CMB heat flux, are largely controlled by the arrival of slabs rather than by the intrinsic dynamics of the lower boundary layer, as is commonly seen in time-dependent mantle convection simulations (e.g. Yuen et al. (1993)). This was clearly quantified by Labrosse (2002), reproduced here in Fig. 1. The time series of heat transport by cold plumes and heat flow across the CMB are highly correlated, whereas heat transported by hot plumes displays similar time-dependence but with a time lag, showing that cold plumes (slabs) control CMB heat flow. A model of a single slab interacting with the CMB also showed some induced plumes (Tan et al., 2002).

The heat flow across the CMB has been a major focus of attention because of its importance in the heat budgets of the mantle and core. One method of estimating it has been to estimate, from their surface uplift, the heat flux associated with hotspots, then assume that plumes reaching the base of the lithosphere carry all of the heat coming from the core, which yields estimates of 6–12% of the surface heat flow (Davies, 1988; Campbell and Griffiths, 1990) — roughly 2.5–5 TW. There are several reasons why this should, however, be regarded as a lower bound, as indicated by several numerical convection studies (Labrosse, 2002; Bunge, 2005; Mittelstaedt and Tackley, 2005; Leng and Zhong, 2008). In simple, basally-heated convection, the heat flux carried by upwellings is half of the global heat flux, because the other half is carried by cold downwellings, which then pool above the CMB absorbing heat from the core- so-called 'slab warming' (Mittelstaedt and Tackley, 2005). Many of the weaker plumes may not reach the base of the lithosphere, instead losing their heat to the interior of the mantle (Malamud and Turcotte, 1999; Labrosse, 2002). In internally-heated convection the geotherm is subadiabatic (e.g. McKenzie et al., 1974; Monnereau and Yuen, 2002; Parmentier et al., 1994), and additionally the adiabatic temperature gradient is steeper for higher temperatures, both resulting in much reduced plume excess temperature (relative to its surroundings) as a plume rises (Bunge, 2005), with Leng and Zhong (2008) finding that the latter effect is the most important. In all of these numerical studies, regardless of geometry or whether compressibility is included, the heat flow across the CMB is a factor of 2 to several times larger than that carried by plumes in the upper mantle. The presence of chemical layering in the deep mantle also has a major effect, as discussed later. An exact determination of CMB heat flow is difficult to make at present because none of the published studies include a realistic variation of physical properties like viscosity, but numbers in the range 7–15 TW are plausible.

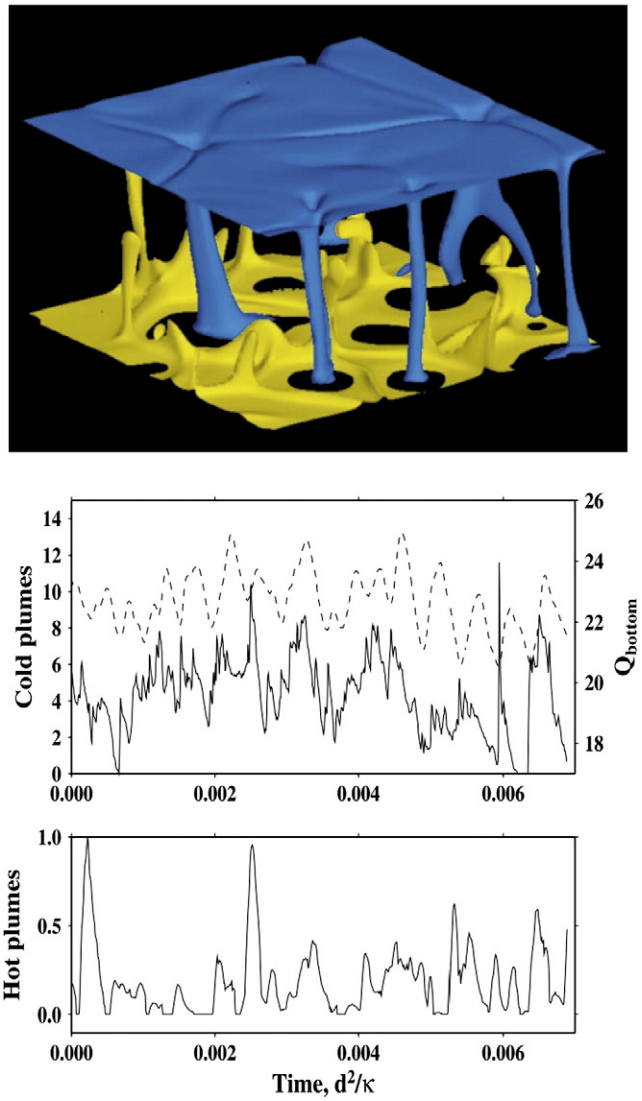

Fig. 1. Thermal convection with mixed basal and internal heating ($Ra = 10^7$ and $H = 20$) and corresponding time series. Isosurfaces are $T = 0.55$ (blue) and $T = 0.8$ (yellow). The time series show heat advection by cold plumes arriving at the CMB (top, solid line, left scale), the heat flux at the CMB (top, dashed, right scale), and heat transport by hot plumes arriving at the top surface (bottom). This shows clearly that the CMB heat flux is controlled by cold plumes arriving rather than hot plumes departing.
Reproduced from Labrosse (2002).

Another constraint on CMB heat flux comes from considering the geodynamo: for a geodynamo to exist, the heat flow from the core must be larger than what can be conducted down the adiabatic gradient. A major uncertainty in this is the thermal conductivity of the core alloy, which is uncertain by a factor of two, and a secondary uncertainty is the power required to drive the geodynamo, which must be added to this. Combined estimates range from 3 to 4 TW (Buffett, 2002) to 8 TW (Gubbins et al., 2004). A third constraint on CMB heat flux comes from observations of post-perovskite phase transition and is discussed in Section 4.4. For further discussion of constraints on CMB heat flow the reader is referred to Lay et al. (2008).

The physics of thermal convection in the deep mantle is complex because of material properties that vary with temperature, pressure, composition and perhaps other things. Viscosity is the material property that varies the most: it depends on temperature (strongly), pressure (less strongly), grain size (when undergoing diffusion creep), stress (when undergoing dislocation creep, which tends to be at high stress), phase, and probably composition. The absolute value of viscosity in the deep mantle is also uncertain. Other material properties that vary with temperature, pressure and composition are thermal conductivity and thermal expansivity, as well as elastic moduli, which are important for seismology.

2.2. Viscosity variation and value

2.2.1. Variation

Substantial variations in viscosity, by many orders of magnitude, are likely to occur in the deep mantle due to variations in temperature, chemistry, phase, grain size and possibly deformation history. The temperature- and pressure-dependence of viscosity is often expressed using an Arrhenius law, such as:

$$\eta(T,p) = A\exp\left[\frac{H(p)}{RT}\right] \quad (1)$$

where T is temperature, p is pressure, A is a constant, H is a pressure-dependent activation enthalpy and R is the gas constant. H is often written in terms of an activation energy E and an activation volume

V as $H(p)=E+pV$, but this is misleading because H is not linearly dependent on pressure (e.g. Ammann et al., 2009; Sammis et al., 1977; Yamazaki and Karato, 2001), which means that in this formulation V is itself pressure-dependent (Sammis et al., 1977; Matas and Bukowinski, 2007).

Estimates for the activation enthalpy $H(p)$ for perovskite at CMB pressure range from ~500 kJ/mol (Yamazaki and Karato, 2001) to 792 kJ/mol (Ammann et al., 2009). To estimate the corresponding viscosity variation over the lower thermal boundary layer, consider that the temperature might, as discussed in Section 2.1, rise from 2400 K above the TBL to 4000 K at the core–mantle boundary, which leads to viscosity decrease by a factor 2×10^4 to 8×10^6. Which of these is more appropriate is potentially important because increased viscosity contrast can lead to a change in regime. At high viscosity contrast, a different type of plume is obtained, in which small-scale convection within the thermal boundary layer (Solomatov and Moresi, 2002) develops faster than the large-scale instability, resulting in a huge plume with sharp sides (Thompson and Tackley, 1998; Ke and Solomatov, 2004). The cases from Thompson and Tackley (1998) are reproduced in Fig. 2.

It is important to note that published numerical models of global mantle convection have always used a much smaller temperature-dependence of viscosity than realistic, typically because the numerical schemes used cannot handle such large variations. Often, global simulations include only depth-dependent viscosity or set the temperature-dependence to some arbitrary factor that is not related to any mineral physics constraint. Thus, while the term "Earth-like convective vigour" is increasingly being used to describe global numerical simulations, the reader should be aware that in no case so far does this also mean an Earth-like viscosity variation with temperature.

Viscosity is also dependent on several other intrinsic or extrinsic quantities:

1. *Dislocation creep*, rather than diffusion creep, can occur at high stress levels, which in this context exist where slabs reach the CMB and are forced to bend (McNamara et al., 2001). Slabs normally have a high viscosity because they are cold, so dislocation creep in the bending slab acts to reduce these high viscosity values.
2. *Post-perovskite*, according to ab initio calculations of atomic diffusion (Ammann et al., 2010) can have an up to ~3 orders of magnitude lower viscosity than perovskite, although its viscosity is highly anisotropic so it is uncertain which direction dominates. If so, then because post-perovskite tends to occur in cold regions, this also reduces the highest values of viscosity in the CMB region, which assists slabs in bending at the CMB, significantly increasing overall convective vigour and heat transport (Nakagawa and Tackley, 2011). This is further discussed in Section 4.2.2.
3. *Grain size* strongly affects the diffusion creep viscosity, with smaller grains facilitating faster creep. Grain size tends to increase with time and decrease with deformation, and may be greatly reduced by recrystallisation when material passes through a phase transition such as perovskite–post-perovskite. The evolution of grain size in the lower mantle is discussed in detail by Solomatov (2001), Solomatov et al. (2002) and Solomatov and Reese (2008); the issue is plagued by uncertainties in the relevant parameters, but it may have some curious effects such as making hot plumes more viscous (Korenaga, 2005).

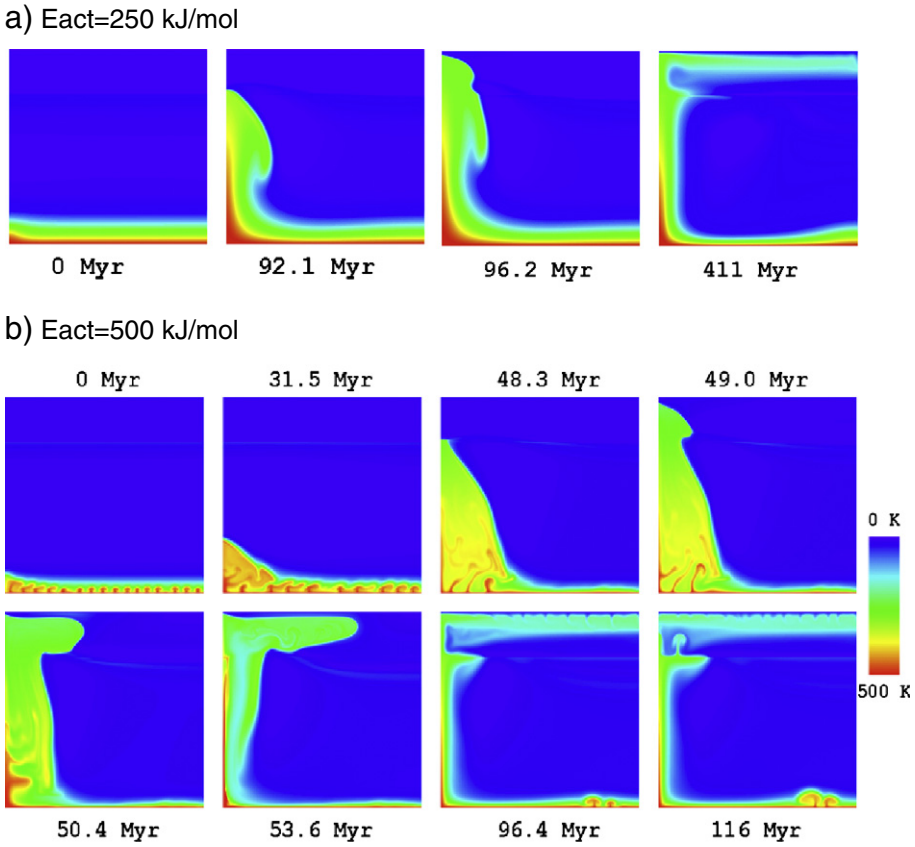

Fig. 2. Development of plumes in a compressible mantle with depth-dependent physical properties and temperature-dependent viscosity with an activation of (a) 250 kJ/mol and (b) 500 kJ/mol. Plotted is superadiabatic temperature. With the larger activation energy, internal convection develops inside the boundary layer and a much larger plume is formed. Reproduced from Thompson and Tackley (1998).

4. *Composition*, which is thought to vary in the deep mantle, may also influence viscosity, although the lack of data on this precludes further discussion.

It has also been proposed that viscosity is substantially reduced during the transition of iron from high spin to low spin (Wentzcovitch et al., 2009; Matyska et al., 2011), which occurs in ferro-periclase at mid-lower mantle pressures (Badro et al., 2003) and is spread over some depth range (Tsuchiya et al., 2006). This proposed viscosity reduction was based on the reduction of effective bulk modulus during the transition. First-principle calculations of atomic diffusion (Ammann et al., 2011) indicate, however, that in fact the spin transition has only a small impact on the rheology.

2.2.2. Absolute value

The value of viscosity above the lower TBL is of great interest because it determines the general convective vigour of the deep mantle. Constraints come from the analysis of postglacial rebound/adjustment (PGR/PGA) data, sometimes in conjunction with rotational data, modelling of geoid and topography based on density anomalies derived from seismic tomography, from mineral physics constraints, and from matching other observations (e.g. heat flow) using modelling. PGA constrains the absolute viscosity whereas geoid/topography modelling only gives a relative profile, unless combined with other constraints such as matching plate velocities.

Viscosity values in the deep mantle derived from PGR and geoid/topography modelling are typically in the range ~few.10^{21}–few.20^{22} Pa.s. For example Peltier and Jiang (1996) derive seven viscosity profile models using a combination of PGA and rotational data, finding deep mantle viscosity in the range 2×10^{21}–7×20^{22} Pa.s., and the related model of Peltier (1996) finds ~3×10^{21} Pa.s above the CMB. King (1995) used a genetic algorithm to derive various viscosity profiles that fit geoid/topography data; in the deep mantle the obtained values were in the range 2–8×10^{21} Pa.s. Mitrovica and Forte (2004) obtained viscosity profiles by inverting a smorgasbord of geophysical data including PGA, free-air gravity, excess ellipticity of the CMB and tectonic plate motions, finding a lower mantle viscosity profile that rises to a peak of ~10^{23} Pa.s at 2000 km depth, dropping to ~10^{21}–2×10^{22} Pa.s above the lower TBL. In the geoid modelling of Steinberger and Calderwood (2006), advected heat flux was used as an additional constraint; resulting deep mantle viscosities for the optimised models were in the range ~6×10^{22}–6×10^{23} Pa.s at 2300 km depth before dropping 2–3 orders of magnitude to the CMB.

In these studies the value of viscosity above the CMB is difficult to interpret because there is some trade-off between the viscosity above the lower TBL and the viscosity reduction inside the TBL. By examining fits to rotational data Peltier and Drummond (2010) demonstrated this trade-off very effectively. An example of a good-fitting combination from their study is 10^{18} Pa.s inside the TBL and 10^{22} Pa.s above it.

Mineral physics constraints on lower mantle rheology were discussed by Yamazaki and Karato (2001). They considered several different models of lower mantle H(p) including a homologous temperature scaling and an elastic strain energy model, finding that when combined with a reasonable geotherm, the viscosity of the lower mantle does not increase dramatically with pressure, and could be in the range 10^{20}–10^{22} Pa.s in the deepest part. Recently, Ammann et al. (2010) calculated a lower mantle viscosity profile based on H(p) from the ab initio calculations of Ammann et al. (2009), finding a range of 10^{22}–10^{24} Pa.s above lower TBL. One uncertainty with mineral physics-based viscosity estimates is that the diffusion creep viscosity is strongly dependent on the grain size, which is not known. Another key issue is that there are two main phases in lower mantle rock with quite different viscosities. The less abundant (~20%) phase magnesiowüstite (also known as ferropericlase) has a much lower viscosity, by perhaps a few orders of magnitude, than the dominant (~80%) lower mantle phase perovskite, and therefore the effective viscosity of the lower mantle depends on which of these phases dominates the overall viscosity. If the strong perovskite phase forms as interconnected matrix then it will dominate, but if the perovskite grains are separated by a film of MgO, then MgO could dominate. This could well evolve with deformation. In laboratory experiments Yamazaki et al. (2009) observed a dihedral angle that would lead to an interconnected network of weak ferropericlase, with the interconnectivity increasing with temperature, although Yoshino et al. (2008) found that the measured electrical conductivity of such a mixture is more consistent with no interconnection of ferropericlase. Clearly, the issue requires more study.

In summary, the viscosity of the deep mantle above the TBL in the perovskite stability field is uncertain to ~1 order of magnitude, but a value of ~10^{22} Pa.s seems to fit almost all observational and mineral physics constraints.

2.3. Thermal conductivity

For some time there has been agreement that thermal conductivity increases with pressure (e.g., Anderson, 1987; Osako and Ito, 1991). There are two components to the thermal conductivity: (i) a lattice (phonon) part, which increases with pressure but decreases with temperature, and (ii) a radiative part, which increases strongly with temperature, and is probably small in most of the mantle but may become important at the high temperatures in the deep mantle.

Whether the radiative conductivity is important is highly uncertain, and depends on how well infrared radiation can pass through the rock. This might be affected by the iron spin transition, which was argued by Badro et al. (2004) to greatly increase the thermal conductivity so as to cause "nonconvecting layers in the mantle", although a quantitative value of conductivity was not given. The influence of various factors on the radiative conductivity was recently studied in laboratory experiments by Goncharov et al. (2009), who found that the spin transition has a relatively small effect, with increasing amount of iron resulting in higher absorption and post-perovskite having a higher absorption than perovskite. Thus, at the moment it appears that the radiative component is small.

Another complexity is that the thermal conductivity varies widely for different minerals: magnesiowüstite has a much higher thermal conductivity than perovskite. Thus, as with viscosity the question becomes how to average them appropriately to obtain the bulk conductivity of the aggregate.

A model that combines all these is in Hofmeister (1999), and several modelling papers have used this formulation. Recent experimental and first principles work has refined our knowledge, however. Hofmeister (2008) presents a combined model incorporating both minerals and both phonon and lattice conductivity. Along a mantle adiabat, the phonon thermal conductivity is calculated to reach up to 17 W/m-K for perovskite and ~50 W/m-K for magnesiowüstite. The radiative conductivity increases from 1 to 5 W/m-K. The combined conductivity of 80% perovskite and 20% magnesiowüstite ranges from 12 W/m-K at the top of the lower mantle to 28 W/m-K in the deepest mantle.

These high values of phonon conductivity for MgO are supported by first principles calculations by de Koker (2010), who finds values of up to ~36 W/m-K, Tang and Dong (2010), who find values as large as 35–50 W/m-K, and Stackhouse et al. (2010), who find values of ~30 W/m-K, all above the lower TBL. For perovskite there is, however, disagreement about its phonon thermal conductivity in the deep mantle. Experimental data indicates high values: Goncharov et al. (2009) found 10–35 W/m-K (although it is stated that "uncertainty is large") and Ohta (2010) found ~18 W/m-K, while the first principles calculations of de Koker (2010) find a value of 2.5 W/m-K. The latter study calculates the overall thermal conductivity of 20% MgO + 80% $MgSiO_3$ in the deep mantle to be 5.9 W/m-K., while Ohta (2010) calculates 20–22 W/m-K for 16% MgO + 84% $MgSiO_3$. Manthilake et al. (2011) found that the thermal conductivity is strongly dependent on the presence of impurities: even small amounts of Fe or Al can reduce the thermal conductivity of

perovskite or magnesiowüstite by ~50% compared to the pure Mg endmember. They calculate an aggregate thermal conductivity above the lower TBL of 18 W/m-K for the pure endmember with 20% MgO + 80% $MgSiO_3$ but 9 W/m-K for more realistic compositions containing some Fe.

In summary, plausible values for deep mantle thermal conductivity are bracketed by the ~28 W/m.K calculated by Hofmeister (2008) and 5.9 W/m.K calculated by de Koker (2010) — a factor of almost 5 difference, with the main uncertainty being the thermal conductivity of perovskite and a secondary uncertainty being the radiative conductivity. Values towards the lower end of this range (e.g. 9 W/m-K) are preferred when the influence of impurities is taken into account (Manthilake et al., 2011).

2.4. Thermal expansivity

Thermal expansivity decreases with increasing pressure. Almost all mineral physics papers that calculate the expansivity at CMB pressures find values of $1.0–1.2\times10^{-5}$/K (e.g., Anderson et al., 1992; Chopelas and Boehler, 1992; Katsura et al., 2010; Kombayashi et al., 2008; Mosenfelder et al., 2009; Tsuchiya et al., 2005). Occasionally, lower values will be given, such as 0.6×10^{-5}/K inferred from the study of (Katsura et al., 2009). Thermal expansivity is also mildly dependent on temperature, but not enough to justify including temperature-dependence in numerical studies of deep mantle dynamics (although Ghias and Jarvis (2008) found that it has some influence on surface heat flux and velocity).

In modelling studies by geodynamicists it is quite common to not include pressure-dependence and assume much higher values of thermal expansivity such as $2.0–3.0\times10^{-5}$, which are appropriate for the top of the lower mantle but not the deepest part. This causes an overestimation of thermal buoyancy in the lower TBL, so such studies must be interpreted and rescaled accordingly.

2.5. Dynamical effect of depth- and temperature-dependent properties

Viscosity, thermal conductivity and thermal expansivity all change with increasing depth (pressure) in such a way as to decrease the convective vigour in the deep mantle. Specifically, and as discussed in 2.2–2.4, thermal expansivity decreases with pressure, while thermal expansivity and viscosity increase with pressure.

Many mantle convection modelling studies since the early 1990s have shown that including depth-dependence of one or more of these three physical properties generates large-scale features in the deep mantle and increases the horizontal wavelength of convection (Hansen et al., 1991; Yuen et al., 1991; Balachandar et al., 1992; Cserepes, 1993; Hansen et al., 1993; Reuteler et al., 1993; Hansen and Yuen, 1994; Bunge et al., 1996; Tackley, 1996; Moser et al., 1997). A recent study to investigate the influence of such effects is Monnereau and Yuen (2010), shown in Fig. 3. This shows the influence of different increases of thermal conductivity with depth, other parameters being the same. A large increase of thermal conductivity with depth results in huge plumes being generated in the deep mantle, and a general increase in mantle temperature at all depths. Extreme variations of thermal expansivity and conductivity combined with the endothermic phase transition at 660 km depth may result in broad lower mantle plumes that feed multiple narrow upper-mantle plumes (Matyska and Yuen, 2007).

Temperature-dependent viscosity acts in the opposite sense, counteracting this tendency towards large upwellings. For example, Matyska and Yuen (2006) show cases that have temperature-dependent thermal conductivity, reproduced here in Fig. 4. When viscosity is only depth-dependent, this temperature-dependent thermal conductivity gives similar results to the depth-dependent thermal conductivity discussed above, resulting in huge plumes in the deep mantle (Fig. 4 left panel). When, however, temperature-dependent viscosity is also included, this counteracts the effect of temperature-dependent thermal conductivity, causing smaller, narrower, more time-dependent plumes (Fig. 4 middle panel). Thus, for making accurate predictions about the deep Earth it is necessary to include realistic variations of material properties, in particular viscosity, with both temperature and pressure. Many of the published simulations do not do this because they are intended to give theoretical guidance about the influence of different parameters rather than be realistic representations of the actual Earth. Calculations that are intended to combine realistic variation of physical parameters were shown in Schubert et al. (2004), reproduced here in Fig. 5. In the regional model (left panel), a reasonable variation of material properties with depth is assumed as given in Tackley (2002), with a viscosity variation with temperature and pressure based on Yamazaki and Karato (2001) and a value of 10^{22} Pa.s just above the lower thermal boundary layer. A cluster of narrow plumes forms. The large-scale model (first presented by Hansen and Yuen, AGU 2002) has a decrease of thermal expansivity with depth by a factor of 3 and both depth- and temperature-dependent viscosity, and has several small plumes forming a plume cluster. From these calculations, it seems clear that plume clusters are the preferred mode of focussed upwelling for purely thermal convection.

In summary, the deep mantle values of viscosity, thermal expansivity and thermal conductivity as well as their variation with temperature have a first-order influence on deep mantle thermally-driven dynamics. High viscosity, conductivity and low expansivity result in large-scale structures, but this is counteracted by temperature-dependent viscosity, which probably varies by 4–6 orders of magnitude across the lower TBL and results in plume clusters, unless its temperature-dependence is so large that convection with the TBL results in internal convection and the formation of 'megaplumes'. The arrival of downwelling slabs at the CMB controls the location of plumes and the time-dependence of CMB heat flow. Uncertainty in physical properties precludes making precise calculations.

3. The role of compositional variations

3.1. Seismological observations

Several observations in global seismic tomographic models indicate the presence of compositional variations in the deep mantle. These are, that the correlation between P- and S-wave velocities drops in the lowermost mantle (Saltzer et al., 2001; Becker and Boschi, 2002; Simmons et al., 2010), the correlation between bulk sound and S-wave anomalies becomes negative in the deep mantle (Su and Dziewonski, 1997; Antolik et al., 2003; Kennett and Gorbatov, 2004; Saltzer et al., 2004), and the amplitude ratio between S- and P-wave velocity anomalies becomes large in the deep mantle (Robertson and Woodhouse, 1996; Masters et al., 2000; Karato and Karki, 2001; Ritsema and Van Heijst, 2002). All of these cannot be explained purely by temperature variations, and require compositional variations as well (although in the lowest ~200 km the post-perovskite transition could cause such a signature as discussed in Section 4.3). Recently, Della Morra et al. (2011) showed that the resolution of seismic tomographic models is sufficient to resolve these characteristics.

The above tomographic models did not use data that can directly constrain density. Seismic inversions that use normal mode splitting functions can, however, directly infer density variations, albeit only at long wavelength, and also find a strong influence of compositional variations in the deepest mantle (Ishii and Tromp, 1999; Trampert et al., 2004; Deschamps et al., 2007).

As discussed in more detail below, the form of compositional heterogeneity that is most compatible with seismological observations as well as other constraints is isolated 'piles' of dense material, as first modelled in 2-D by Hansen and Yuen (1988, 1989) and in 3-D by Tackley (1998, 2002). In the present-day Earth, two 'piles' are located under Africa and the Pacific, and are evident in tomographic models

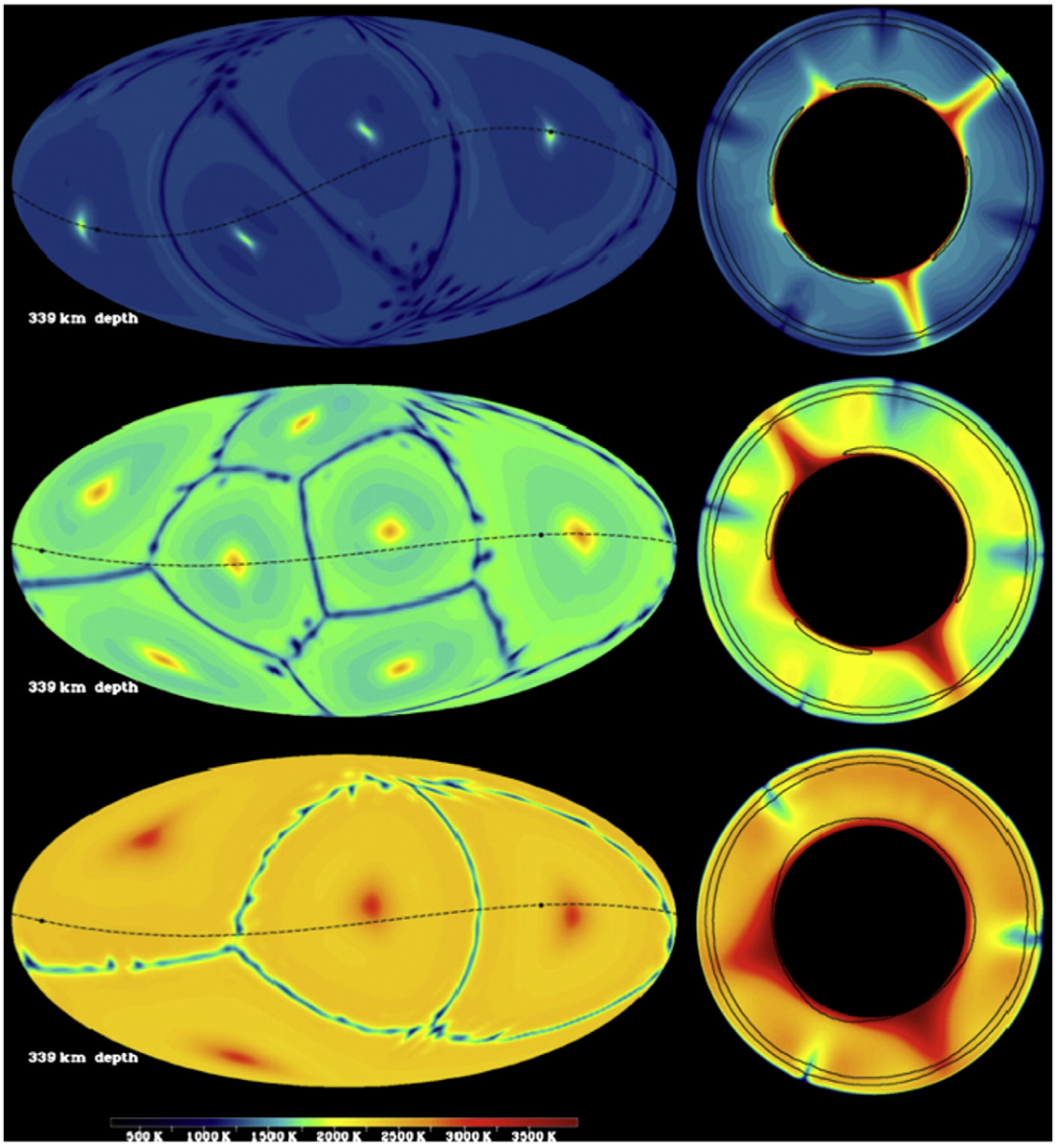

Fig. 3. Temperature fields from 3-D spherical simulations with various different increases of thermal conductivity with depth but similar surface and CMB heat fluxes. The maps on the left are at 330 km depth, while the slices on the right on the indicated lines. The thermal conductivity rises from 3 W/mK at the surface to 5, 10 or 30 W/mK at the CMB (top to bottom cases).
Reproduced from Thompson and Tackley (1998).

by their low shear wave velocity, which has led to the cumbersome acronym LLSVP (large low seismic shear-velocity province). Seismic waveform modelling indicates that these have sharp, steep sides (Ni et al., 2002; Wang and Wen, 2004; Ni et al., 2005; Wang and Wen, 2007; He and Wen, 2009).

Two obvious questions arise: (i) where does this dense material come from? and (ii) what is its dynamical effects? These are addressed in the next two sections.

3.2. Origin of the dense material

There are several possible origins of dense material in the deep mantle, which fall into two main categories: generated over time, or 'primordial', i.e., arising from very early processes.

Mechanisms for generating a primordial layer are fractional crystallisation of a magma ocean (Solomatov and Stevenson, 1993; Abe, 1997), subduction of a very early crustal layer (Tolstikhin et al., 2006) or an early KREEP-like liquid (Boyet and Carlson, 2005), or "upside-down differentiation" (Lee et al., 2010), in which melt that formed deep in the hot, early upper mantle could have segregated downwards rather than upwards, then solidified and sunk into the deepest mantle.

A recently-proposed mechanism for generating deep, dense material over time is the crystallisation of a "basal magma ocean" (BMO) (Labrosse et al., 2007). In this scenario, the entire mantle started off molten and crystallised from the middle, rather than the bottom as previously thought (Solomatov and Stevenson, 1993; Abe, 1997). Thus, the deep mantle would have been partly molten for much of Earth's history, with some pockets of remnant partial melt left at the present day in the form of Ultra-Low Velocity Zones (ULVZs), discussed in Section 5. Over time, fractional crystallisation would have changed the composition of the remaining liquid and of the solid that progressively

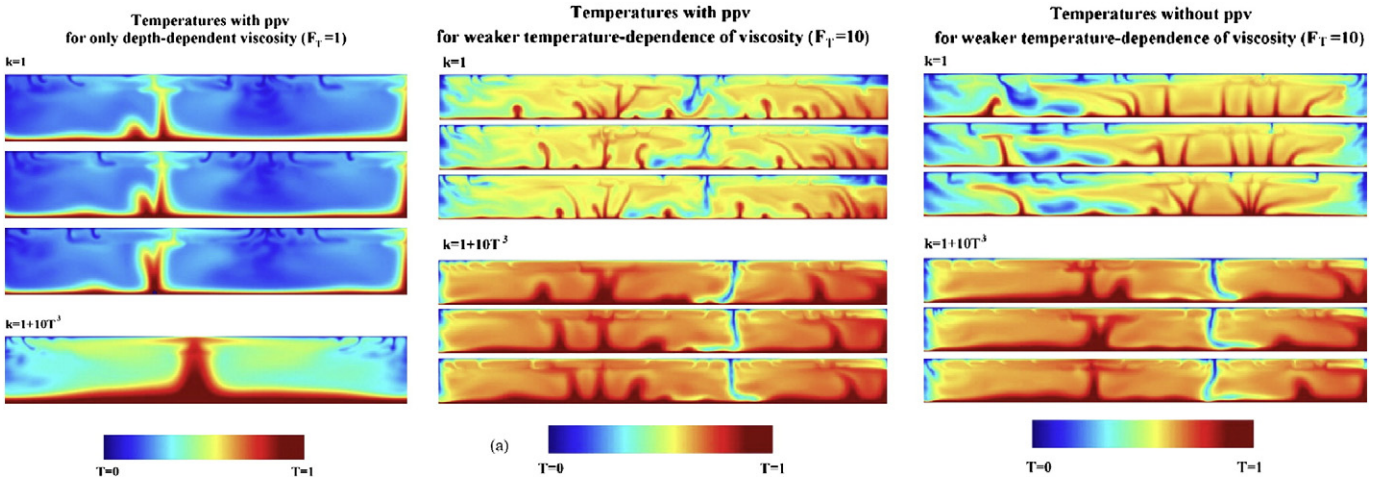

Fig. 4. 2-D convection models with various variations in physical properties. The upper calculations have constant thermal conductivity $k=1$, whereas the lower calculations have temperature-dependent thermal conductivity $k=1+10\,T^3$. The three panels show calculations with (left) depth-dependent viscosity and post-perovskite (middle) depth- and T-dependent viscosity and post-perovskite, (right) depth- and T-dependent viscosity without post-perovskite.
Reproduced from Matyska and Yuen (2006).

crystallised, such that the crystallising solid would have become increasingly iron-rich and therefore dense.

The mechanism for generating deep, dense material over time that has received the most attention by the modelling community is recycling and segregation of oceanic crust. The potential importance of this is related to the total volume of MORB that has been produced over geological time. The production rate at the present day and during the recent past is well quantified (e.g, Phipps Morgan, 1998; Stacey, 1992). If this was constant for the whole of Earth's history, then the total volume of crust produced was 10% of the mantle volume (Xie and Tackley, 2004b). Most likely, however, convection and oceanic crust production was more vigorous in the past. For simple, internally-heated convection the surface velocity scales as the square of internal heating rate, and two studies (Davies, 1980; Phipps Morgan, 1998) have argued that in plate tectonics convection the oceanic plate velocities and hence crustal production rate should scale in the same way. If that is the case, then the volume of oceanic crust produced corresponds to 53% of a mantle volume (Xie and Tackley, 2004b). There is much uncertainty over these estimates, but they serve to show that the volume produced is substantial and easy enough to explain the seismologically-inferred volume of the dense regions (Hernlund and Houser, 2008). It was recently suggested that tonalite–trondhjemite–granite (TTG) continental crust may be subducted to the CMB region (Komabayashi et al., 2009; Senshu et al., 2009), but the volume of this is expected to be much smaller than the volume of MORB subducted over geological time discussed above.

Once a slab reaches the CMB, some fraction of its basalt may separate and remain above the CMB, as shown in the early laboratory experiments of Olson and Kincaid (1991). Some recent simulations of this process (Tackley, 2011) are shown in Fig. 6, for slab segments arriving with three different dip angles. First, slabs have a tendency to rotate basalt-side down because of the differential buoyancy of basalt and harzburgite. Dense material above the CMB is pushed aside, allowing the slab to reach the CMB and rapidly heat up. Plumes arise at its edges, which are also the edges of the dense regions, and have a tendency to contain harzburgitic material, which is compositionally buoyant and therefore wants to rise as soon as it heats up. Much of the basaltic material peels off the slab (particularly if the basalt side touches the CMB) and may subsequently join the layer or be entrained by plumes. The presence of an existing layer increases the fraction of slab basalt that remains near the CMB (Tackley, 2011).

There have been several numerical studies that address the global, long-term evolution of this process, starting with Christensen (1989) and Christensen and Hofmann (1994) and continuing with different geometries and different assumptions in 2-D (Davies, 2002; Ogawa, 2003; Xie and Tackley, 2004a,b; Brandenburg et al., 2008), and in 3-D spherical (Huang and Davies, 2007; Nakagawa et al., 2009, 2010) geometries. Fig. 7 shows a typical case, from Nakagawa and Tackley

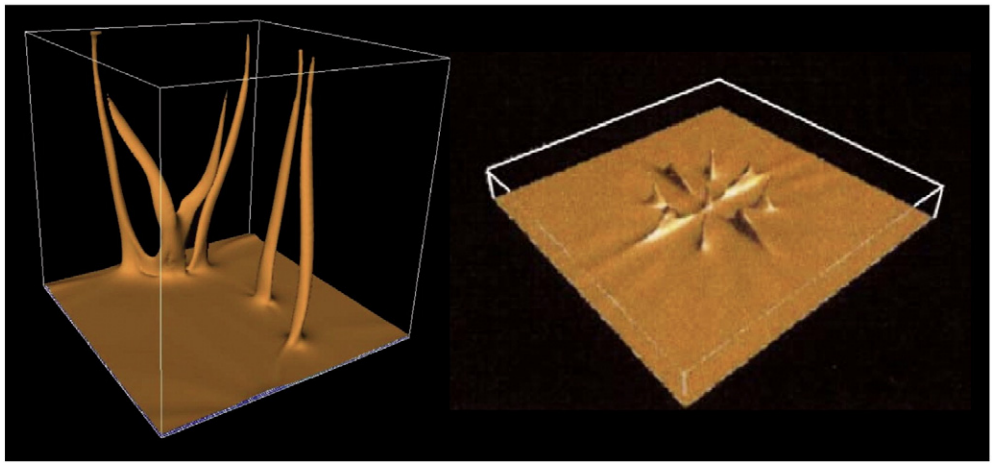

Fig. 5. 3-D convection models with temperature- and depth-dependent viscosity and depth-dependence of other physical properties, showing the formation of plume clusters.
Reproduced from Schubert et al. (2004).

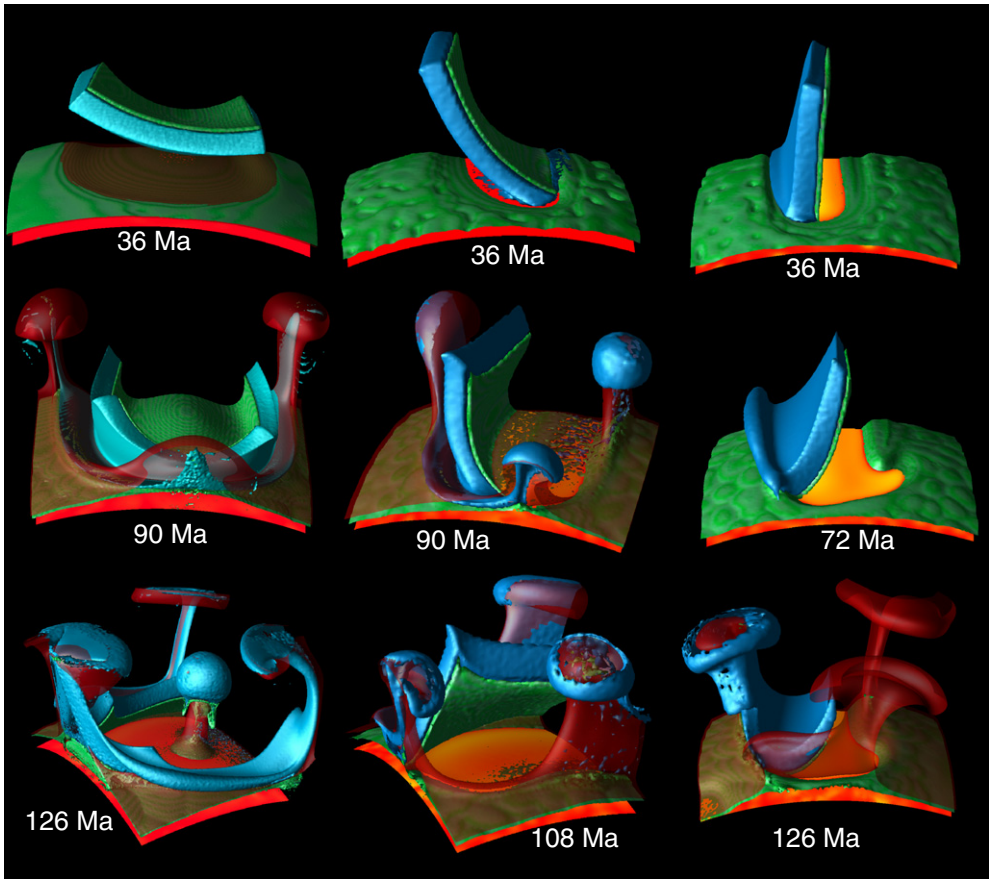

Fig. 6. Interaction of a compositionally-stratified slab section with a layer at the CMB. Each column shows a time sequence for a different initial slab dip angle. blue = harzburgite, green = MORB, red = hot temperature. Slabs tend to rotate basalt-side down. Plume heads containing buoyant depleted material are formed soon after the slab reaches the CMB; subsequent plume tails may entrain MORB. A substantial fraction of the MORB initially on the slab joins the dense layer via various different mechanisms.
Reproduced from Tackley (2011).

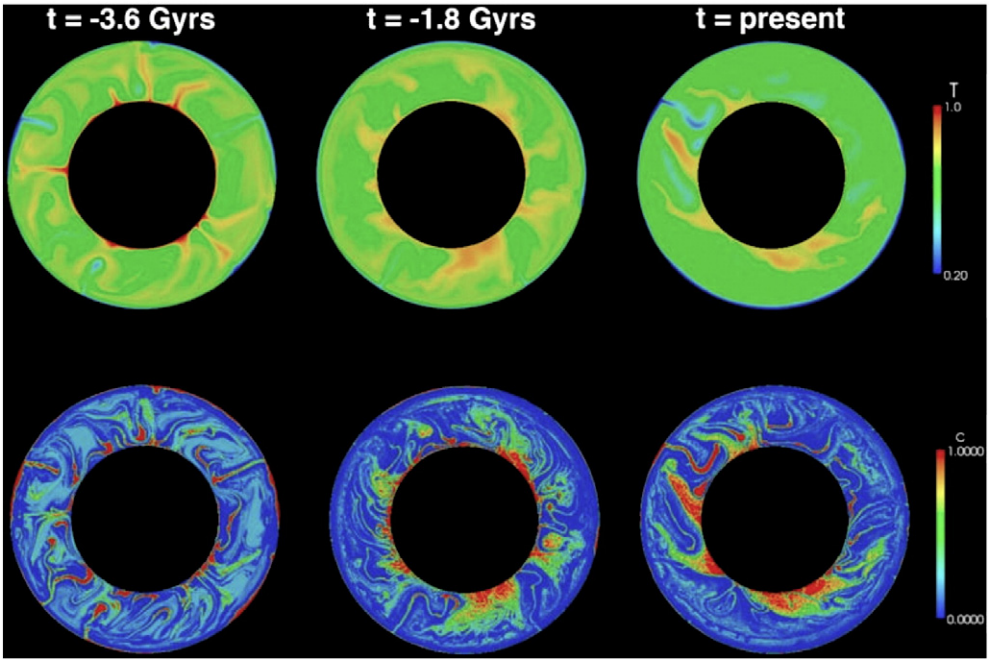

Fig. 7. The formation of a deep, dense layer by segregation of subducted MORB in a 2-D spherical annulus. The top row shows potential temperature (red = hot to blue = cold) and the bottom row shows composition (red = MORB and blue = harzburgite). The density contrast between MORB and harzburgite near the CMB is 1.35%.
Reproduced from Nakagawa and Tackley (2010).

(2010). The general finding is that a dense layer forms that is mostly but not entirely made of MORB, and some fraction of the subducted MORB remains in this layer. The layer does not have a sharp top, but rather a compositional gradient, and may develop a range of irregular structures including some with sharp vertical sides and even tilted (Fig. 7). Typically, after ~2 Ga the amount of material in this layer reaches an equilibrium, at which the addition of new MORB is balanced by the entrainment of existing layer material into upwellings. The material in the layer becomes hot, giving a super-adiabatic lower mantle geotherm (Nakagawa and Tackley, 2005b).

It is encouraging that these various global studies obtain similar behaviour and resulting thermo-chemical structures despite some quite different modelling assumptions and numerical methods. As shown by Christensen and Hofmann (1994), the volume of segregated crust depends mainly on two factors: the density anomaly of MORB in the deep mantle, and the Rayleigh number (Ra), which is a nondimensional measure of the convective vigour (Rayleigh, 1916). It is obvious why denser MORB leads to more settling. Less intuitive is that higher Rayleigh number leads to less settling, with the volume of material in the deep layer scaling approximately as $Ra^{-2/3}$ (Christensen and Hofmann, 1994; Brandenburg and van Keken, 2007). This could be related to more rapid entrainment and/or the difference in thermal boundary layer thickness. Two obvious questions follow: what is the density anomaly of MORB in the deep mantle, and what is the appropriate Rayleigh number? The Rayleigh number is a combination of various uncertain physical properties discussed earlier (with viscosity and thermal conductivity having the highest uncertainty) and will not be further discussed here.

The density anomaly of MORB at the CMB has variously been calculated to be from slightly negative to as much as 5% positive. In early papers (e.g. Ringwood, 1990) the focus was on the transition zone and top of the lower mantle, but it appeared that MORB would remain denser throughout the lower mantle. However, Kesson et al. (1998) calculated that at CMB pressures MORB is actually slightly less dense than pyrolite, by 30 kg/m^3, although slightly (by 11 kg/m^3) denser than depleted residue. This was reinforced by Ono et al. (2001), who calculated a density crossover such that MORB is dense at the top of the lower mantle but less dense than pyrolite at the CMB. Subsequent papers have, however, found that MORB is denser than pyrolite, with Guignot and Andrault (2004) finding it 25–95 kg/m^3 denser and Hirose et al. (2005) finding it 200–300 kg/m^3 denser throughout lower mantle, which corresponds to 3.5–5.3% at the CMB. Recently, Ricolleau et al. (2010) measured the phase assemblages and densities of a natural MORB sample at up to 89 GPa, then calculated the density profile of MORB for various compositions and temperature profiles. Depending on exact composition, they found that thermally-equilibrated MORB is between 0.5 and 2% denser than PREM over the entire lower mantle range. The influence of exact MORB composition on segregation of MORB above the CMB was studied by Nakagawa et al. (2010) in 3-D spherical convection simulations incorporating a self-consistent mineralogical approach, and was indeed found to have a strong influence. More exotic combinations of subducted material are possible, and have been speculated by Komabayashi et al. (2009).

Attempts to match one-dimensional seismic profiles of the lower mantle (like PREM (Dziewonski and Anderson, 1981)) with candidate temperature- and compositional-profiles, have often indicated a preference for some gradual MORB enrichment in the deep mantle, as well as a super-adiabatic temperature profile, which is a characteristic of deep mantle layering as mentioned above. The basic problem is that according to our best knowledge of the relevant physical properties, adiabatic pyrolite does not match PREM: its density, for example, increases too rapidly with depth (Ricolleau et al., 2009). The inversions of Matas et al. (2007) prefer a superadiabatic temperature gradient and a deep mantle composition that is consistent with slight MORB enrichment. Accounting for uncertainties in properties, Cobden et al. (2009) also prefer MORB enrichment going deeper into the lower mantle. Considering electrical conductivities also results in a preference for MORB enrichment in the deep mantle (Ohta et al., 2010). Locally there is some evidence for the presence of MORB from inversion of seismic waveforms for local radial structure in the western Pacific (Konishi et al., 2009). There is no universal agreement, however; for example while the seismological-mineral physics inversion of Khan et al. (2008) also finds a superadiabatic temperature profile in the lower mantle and a lower mantle enrichment in FeO, it finds lower mantle depletion in SiO_2, opposite to what would be expected for MORB although similar to what would be produced by crystallisation of a dense basal magma ocean (Nomura et al., 2011).

3.3. Dynamical behaviour of dense material

3.3.1. Parameters

To characterise the dynamical behaviour of a layer of dense material, two nondimensional parameters are relevant. The first is the Lewis number, which is the ratio of chemical diffusivity κ_T to thermal diffusivity κ_C:

$$Le = \frac{\kappa_T}{\kappa_C} \tag{2}$$

and is so large (between 10^8 (Hansen and Yuen, 1989) and 10^{13} (Kellogg and Turcotte, 1986)) that chemical diffusion can be neglected when considering the dynamics of large-scale accumulations of dense material.

The second and most important parameter is the chemical buoyancy ratio, which is the ratio of chemical density contrast $\Delta\rho_C$ to thermal density contrast $\Delta\rho_T$:

$$B = \frac{\Delta\rho_C}{\Delta\rho_T} = \frac{\Delta\rho_C}{\rho\alpha\Delta T} \tag{3}$$

where ρ is density, α is thermal expansivity and ΔT is the temperature contrast. In a simple convecting system with constant properties a number of laboratory and numerical studies (Richter and Johnson, 1974; Richter and McKenzie, 1981; Christensen, 1984; Olson and Kincaid, 1991; Montague and Kellogg, 2000) have shown that if ΔT is the temperature drop across the whole mantle then the dense layer has long-term stability if $B>1$, remains layered but with large layer topography for $1>B>0.5$, but is unstable to rapid overturn and mixing if $B<0.5$ (Davaille, 1999a,b; Le Bars and Davaille, 2002, 2004a,b). These regimes are summarised in a domain diagram in Fig. 8. If ΔT is taken to be the temperature drop over the lower TBL rather than the whole mantle then these numbers must be adjusted accordingly. In the actual mantle α decreases with pressure and ρ increases with pressure; the appropriate values to use are those corresponding to the top of the dense layer.

3.3.2. Topography and planform

The topography on the dense layer depends on B, Ra, and to a lesser extent, the layer thickness (Fig. 8). The topography on a layer interface decreases with increasing Ra, approximately as $Ra^{-1/3}$ (Gurnis and Davies, 1986; Tackley, 1998). The effective Ra of the deep mantle is quite low because of depth-dependent viscosity and other parameters, which allows large interface fluctuations to occur, as shown in 3D calculations (Tackley, 1998; Tackley, 2002). If topography is larger than the layer thickness, then the dense material does not cover the entire CMB, but displays either ridges or discontinuous piles or hills, depending on various parameters. The dense material is swept along by the thermally-driven mantle flow, away from downwellings and accumulating under upwellings (Hansen and Yuen, 1988, 1989). 3-D cartesian calculations (Tackley, 1998; Tackley, 2002) found that the long-term solution is ridges/spokes. Spherical geometry Boussinesq calculations (Oldham and Davies, 2004) indicated a greater tendency

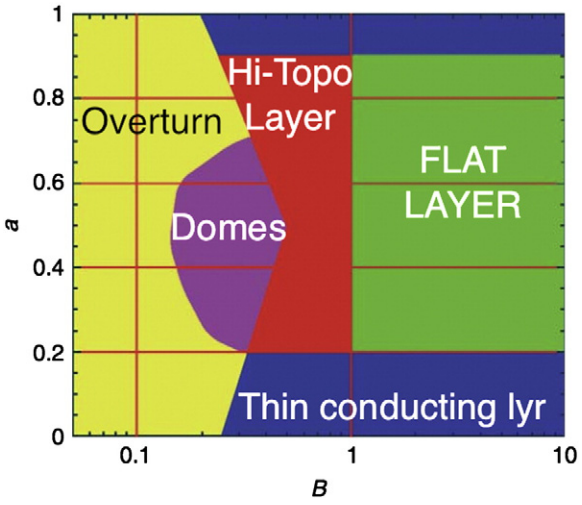

Fig. 8. Domain diagram for the behaviour of thermochemical convection as a function of buoyancy ratio B and initial depth of dense layer a, as determined by laboratory experiments (Davaille, 1999b; Davaille et al., 2002; Le Bars and Davaille, 2002, 2004a,b). Green, flat layers; red, large topography layers; pink, transient oscillating domes; blue, thin non-internally convecting layer progressively entrained by thermochemical plumes; yellow, rapid overturn.
Reproduced from Le Bars and Davaille (2004b).

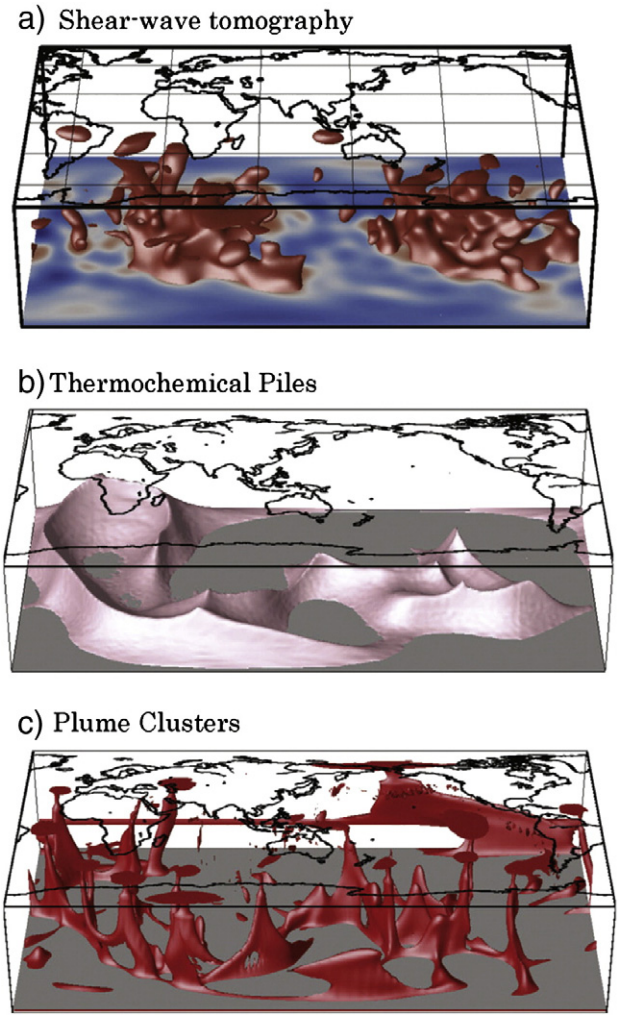

Fig. 9. Comparison of (A) low shear velocity anomalies in the seismic tomographic model S20RTS (Ritsema et al., 1999; Ritsema et al., 2004) with (B) thermo-chemical piles from a dynamical, thermo-chemical calculation and (C) plume clusters from a purely thermal dynamical calculation.
Reproduced from Lassak et al. (2010).

for isolated piles. A viscosity contrast between the layers makes a large difference. McNamara and Zhong (2004b) showed that temperature-dependent viscosity leads to linear piles that are swept around and spread through the entire lower mantle, whereas composition-dependent viscosity in which the dense material is more viscous leads to isolated round 'superplumes', particularly with viscosity contrasts as large as factor 500. Some calculations have been designed to replicate present-day Earth by specifying plate motions from plate reconstructions. McNamara and Zhong (2005) found that structures similar to those seismologically observed under Africa and the Pacific were generated. Specifically, Earth's subduction history tends to focus dense material into a ridge-like pile beneath Africa and a relatively more rounded pile under the Pacific Ocean, which is arguably consistent with seismic observations (Bull et al., 2009). Fig. 9 (from Lassak et al. (2010)) shows a comparison of one of these thermo-chemical convection calculations and the seismic tomographic model of Ritsema et al. (1999) and Ritsema et al. (2004), with a purely thermal model that displays plume clusters also included.

3.3.3. Time evolution

The evolution of a primordial layer is time-dependent. With time, entrainment of the lower layer into the upper layer, and also the upper layer into the lower layer, reduces the density contrast hence B, which may lead to changes in the behaviour. If, as seems likely, the lower layer is thinner then this entrainment is asymmetric and the lower layer shrinks with time, as discussed in Section 2.4. The combination of decreased size and decreased B can lead to changes in the planform and behaviour with time, as illustrated in Fig. 10 from Le Bars and Davaille (2004b). The right column of Fig. 10 shows a sequence from a laboratory experiment, showing how an initial flat layer can evolve into high-topography domes, eventually with blobs, filaments, and a thin remaining layer at the bottom. These are compared (left column) to various cartoon models of the mantle summarised by Tackley (2000).

A systematic study of the influence of various parameters on the long-term behaviour of a primordial dense layer in compressible mantle convection was performed by Deschamps and Tackley (2008, 2009), focussing particularly on solutions that match long-wavelength probabilistic seismic tomographic models (Trampert et al., 2004). In Deschamps and Tackley (2008) it was found that the dependence of viscosity on composition and temperature makes a large difference to the solution, with the best-fitting cases having only a small dependence of viscosity on composition (between factor 0.1 and 10) but a large ($\geq 10^4$) thermal viscosity contrast, which acts to increase the stability of the layer (Tackley, 1998). In Deschamps and Tackley (2009) the endothermic phase transition at 660 km depth was found to strongly inhibit mass exchange and help to keep strong compositional heterogeneities in the lower mantle, while internal heating was found to have negligible influence. The solutions that best match probabilistic tomography had a chemical density contrast of 90–150 kg/m^3, a large thermal viscosity contrast, higher viscosity lower mantle, and a Clapeyron slope at 660 km in the range −1.5 to −3.0 MPa/K, a value that is supported by laboratory experiments (Ito and Takahashi, 1989; Akaogi and Ito, 1993; Yu et al., 2007).

3.3.4. Steep sides

As mentioned earlier, in some places sharp, near-vertical sides to the LLVSPs are observed seismically (e.g. Ni et al. (2002)). It is not known whether these steep sides are stable on the ~Ga timescale, or are simply transient features associated with the time-dependent evolution of a dense layer (e.g. as discussed by Davaille (1999a) and later observed in Deschamps and Tackley (2008, 2009)) with timescales of ~100 s Ma. For the long-term case, the conditions necessary to obtain stable steep edges to thermochemical piles were

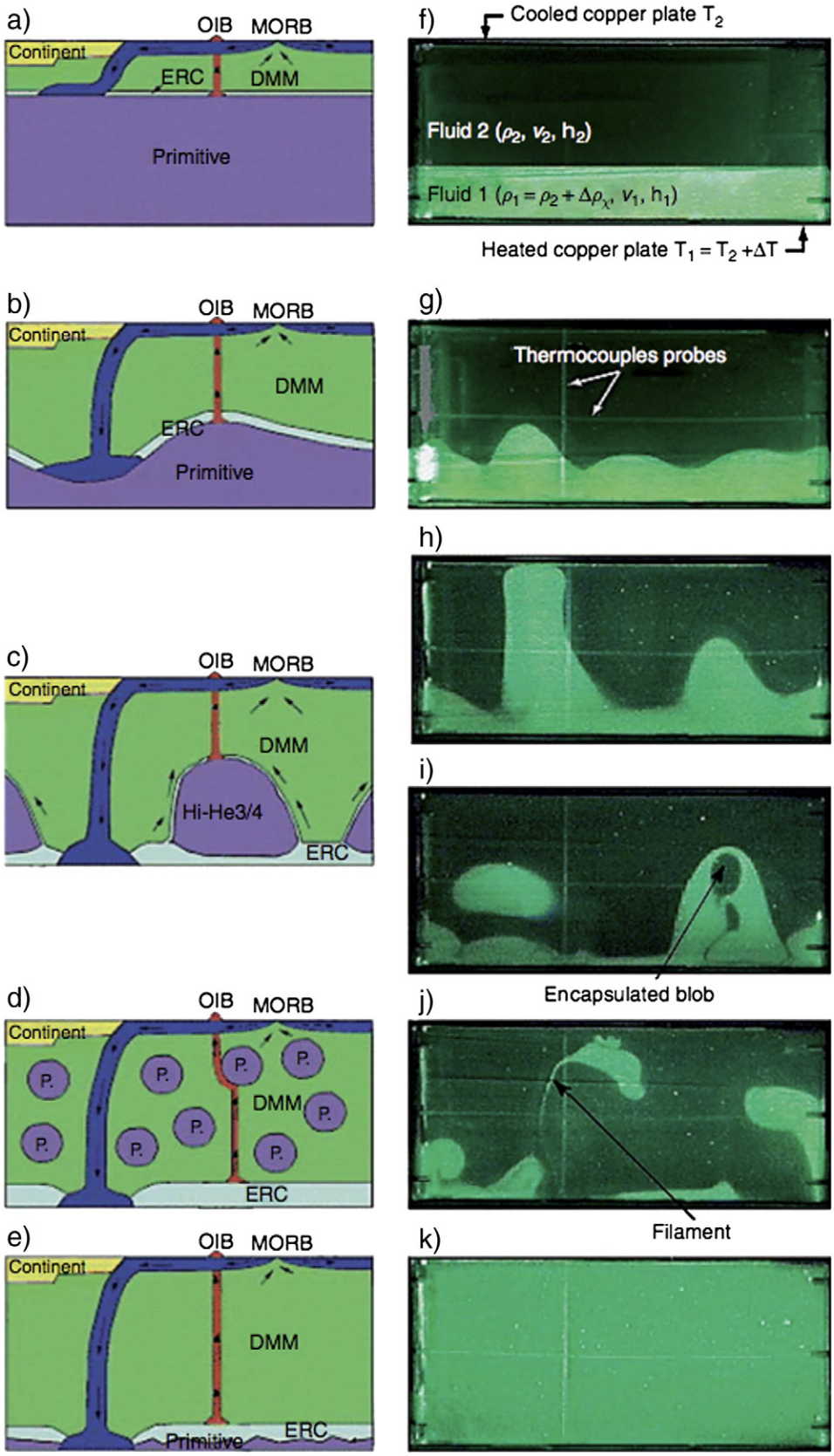

Fig. 10. The time evolution of a laboratory thermo-chemical convection experiment (right column) compared to various mantle models proposed to explain geochemical observations (left column). Cartoons in the left column are from Tackley (2000). (a) Layered at the 660 km discontinuity; (b) deep, high-topography hidden layer (Kellogg et al., 1999); (c) 'piles' (Tackley, 1998) or 'domes' (Davaille, 1999a); (d) primitive blobs (Davies, 1984; Manga, 1996; Becker et al., 1999; du Vignaux and Fleitout, 2001); (e) whole-mantle convection with thin dense layer at the base.
Reproduced from Le Bars and Davaille (2004b).

investigated by Tan and Gurnis (2005, 2007), who found that an increase in chemical density contrast with height above the CMB is necessary. This is because the thermal expansivity increases with height above the CMB, making the top of the piles less stable unless the chemical buoyancy contrast also increases. Whether MORB has this property is uncertain: as discussed earlier some studies have suggested that its density contrast compared to PREM decreases with pressure (Ono et al., 2001) but Hirose et al. (2005) found that its density contrast is approximately constant over the lower mantle and Ricolleau et al. (2010) found that its density contrast is constant or slightly decreasing with pressure, depending on exact composition. Decreasing MORB density contrast with depth has also been included in some numerical simulations in which a layer accumulates over time by segregation of MORB (Xie and Tackley, 2004a,b; Nakagawa and Tackley, 2005a, 2010, 2011) and steep-sided thermo-chemical structures are observed in some of those calculations, such as the one in Fig. 7. The rate at which thermal expansivity changes with depth is very small in the deep mantle (and is exaggerated in Tan and Gurnis (2007) by assuming a linear profile) so the needed difference in compressibility is small. However, as mentioned above, it is not clear that it is necessary for the steep edges to have long-term-stability; they are also observed as transient features in other experiments (e.g. Fig. 10).

3.4. Survival time of dense material

A layer that is dense enough to be stable against rapid overturn nevertheless gets slowly entrained over geological time. There have been several laboratory (Davaille, 1999b; Davaille et al., 2002; Gonnermann et al., 2002; Namiki, 2003), analytical (Sleep, 1988) and numerical (Zhong and Hager, 2003) studies to determine this entrainment rate. The various findings and scaling laws from these studies are compared and reconciled in section 7.10.3.2.1 of Tackley (2007); a brief summary is given here. The various expressions found for entrainment by plumes are generally compatible with the one found by Davaille (1999b):

$$Q = C\frac{\kappa H}{B^2} Ra^{1/3} \frac{1}{1+\Delta\eta/B} \tag{4}$$

where Q is the flux of entrained material, C is an experimentally-determined constant, κ is thermal diffusivity, H is the initial thickness of the lower layer, Ra is the Rayleigh number, $\Delta\eta$ is the ratio of lower layer viscosity to upper layer viscosity and B is the ratio of chemical density difference $\Delta\rho_C$ to thermal density difference $\Delta\rho_T$ given by:

$$B = \frac{\Delta\rho_C}{\Delta\rho_T} = \frac{\Delta\rho_C}{\rho_0 \alpha \Delta T} \tag{5}$$

where ρ_0 is the background density, α is the thermal expansivity and ΔT is the superadiabatic temperature drop across the layer. The time it takes to entrain a dense layer is thus dependent on its density contrast, the viscosity contrast, and the vigour of convection, other things being equal. The density contrast required for a layer to survive over geological time has been calculated by several authors. In many cases these estimates assume an unrealistically high value of deep mantle α such as $2–3\times10^{-5}$/K leading to an unrealistically high value of $\Delta\rho_C$; the estimates were rescaled to a value of 1×10^{-5} in Tackley (2007) and tabulated, as reproduced in Table 1.

When rescaled and compared in this manner, it becomes clear that a chemical density contrast of around 2% or so is needed for a layer to be stable over the age of the Earth, which may be decreased if the dense material has a much lower viscosity (Tackley, 1998; Deschamps and Tackley, 2008).

Table 1
Rescaled estimates of density contrast required for layer survival for 4.5 Ga.

Study	Thickness (km)	Δρ (%)	Δη
Sleep (1988)	100	3.0	1
Davaille et al. (2002)	100	3.5	1
Davaille et al. (2002)	100	2.0	10
Gonnermann et al. (2002)	300	2.0	1
Namiki (2003)	200	2.75	0.01
Zhong and Hager (2003)	1000	1.5	1
Lin and Van Keken (2006a)	>75	>0.5	0.001

3.5. Influence on plumes

Compositional stratification in the deep has a large effect on plumes. An early study (Farnetani, 1997) showed that if plumes form from the top of a dense layer, then their temperature relative to that of their surroundings (the excess temperature) is smaller, helping to explain why the excess temperature inferred for hotspots is relatively small. It also leads to a wider variety of plume forms and dynamics. Farnetani and Samuel (2005) showed that in thermo-chemical convection a great variety of plume shapes and sizes can form simultaneously. This was further supported by the study of Lin and Van Keken (2006b), in which thermo-chemical plumes displayed diverse characteristics that frequently deviated from the classic features of plumes observed in purely thermal convection studies, and also displayed additional time-dependence, for example that might cause multiple flood basalt episodes (Lin and van Keken, 2005).

Plumes normally form from the top of dense piles or ridges in laboratory and numerical experiments of thermo-chemical convection. There has been some debate about whether this increases their fixity relative to plumes forming from a purely thermal boundary layer. Laboratory experiments appeared to indicate that plumes forming from the top of dense ridges are more fixed than purely thermal plumes (Davaille et al., 2002; Jellinek and Manga, 2002), although Davaille et al. (2002) point out that the dense material is swept around by the large-scale flow and thus the dense material acts as a "floating anchor" rather than an absolute anchor. Numerical results, however, found little difference in the fixity of thermo-chemical plumes and purely thermal plumes (McNamara and Zhong, 2004a). The reconciliation of these apparently contradictory results is not clear at present; most likely it depends on the exact parameter range.

Observations indicate that in Earth, present-day plumes (Thorne et al., 2004) and large-igneous provinces (LIPs) (Burke and Torsvik, 2004; Torsvik et al., 2006; Burke et al., 2008; Torsvik et al., 2010) tend to come from the edges of inferred chemically-dense piles (i.e. low-velocity provinces), rather than the tops of them, an apparent difference to laboratory and numerical experiments of thermo-chemical convection. Three factors may, individually or combined, explain this difference:

(1) Previous experiments were not representative of Earth. In thermo-chemical convection calculations that are designed to match present day Earth by specifying historical plate motions as a surface boundary condition (Fig. 9 and Bull et al., 2009; Lassak et al., 2010), cusps from which plumes would be expected to form do appear at the edges of the Pacific and African regions. In local calculations that include realistic compositionally-stratified slabs shown in Fig. 6 from (Tackley, 2011), plumes also tend to form at the edges of regions of dense material (which are also the edges of the slabs).
(2) The top of piles is not a sharp interface. Piles of material that form by the accumulation of subducted MORB (Fig. 7 and Section 3.2) do not have sharp tops, but rather a compositional gradient. Such

a compositional gradient can strongly suppress the formation of plumes (Tackley, 2011).

(3) The dense material is more compressible. Building on earlier findings (Tan and Gurnis, 2005) that steep sides are promoted when the compositional density contrast increases with distance from the CMB (Section 3.3.4), Tan et al. (2011) performed global 3-D spherical models and also found long-lived stable thermo-chemical structures with steep sides and interestingly, plumes coming preferentially from their edges rather than centres.

3.6. CMB topography

Simple considerations indicate that dense material sitting above the CMB is expected to induce negative topography (i.e. a depression) of the CMB, and this was indeed observed in some isoviscous calculations by Hansen and Yuen (1989). In a more realistic system with strongly temperature-dependent viscosity, however, this is incorrect. The 'piles' heat up until their net density anomaly is small, and slabs impinging on the CMB generate more normal stress and stronger negative topography, such that the topography underneath piles is positive relative to the average and topography underneath slabs is negative (Lassak et al., 2007). Purely thermal convection also has negative CMB topography underneath downwellings and positive CMB topography underneath upwellings. Lassak et al. (2010) did a detailed comparison of the calculated CMB topography distribution for the two cases for present-day Earth, making predictions that will require greater seismic resolution to resolve. If the regions where slabs reach the CMB also have a low viscosity due to the presence of post-perovskite (discussed in Section 4.2.2), then the topography under slabs is greatly reduced, reducing the overall CMB topographic variation (Nakagawa and Tackley, 2011).

3.7. Influence on the geodynamo

Because the mantle's viscosity is ~20 orders of magnitude higher than the outer core's, mantle convection determines both the average heat flux and lateral variations of heat flux out of the core, which can influence the existence and the dynamics of the geodynamo. The mean CMB heat flux is strongly influenced by the presence of a dense layer. With no layering, the heat flux can be so large that the inner core grows to much larger than its observed size, unless radiogenic potassium exists in the core (Nakagawa and Tackley, 2004b, 2005a; Nimmo et al., 2004; Butler et al., 2005). A global layer, however, may reduce the heat flux so much that the dynamo shuts off (Nakagawa and Tackley, 2004b, 2005a; Costin and Butler, 2006). A discontinuous layer, as preferred by seismological observations, provides a reconciliation of these problems, reducing the heat flux to reasonable values that are still large enough to power the geodynamo (Nakagawa and Tackley, 2004b, 2005a). This present-day core temperature is insensitive to initial core temperature unless the CMB is completely blanketed by a layer of dense material and for a reasonable core evolution the present-day CMB heat flow is around 9 TW (Nakagawa and Tackley, 2010).

Layering above the CMB also has a dramatic influence on the lateral variation of CMB heat flux. Large lateral variations can prevent a dynamo (Olson and Christensen, 2002), while more moderate variations influence the pattern of core convection (Amit and Choblet, 2010), geomagnetic reversal paths (Gubbins, 1998) and the growth pattern of the inner core (Aubert et al., 2008). 3-D spherical convection calculations (Nakagawa and Tackley, 2008) show that the peak-to-peak heat flux variation is approximately twice the mean heat flux, and that a discontinuous dense layer results in a bimodal heat flux distribution, which is influenced by the viscosity of post-perovskite as discussed later.

4. Role of the post-perovskite phase transition

4.1. Background

The phase transition from perovskite to post-perovskite was discovered in 2004 (Murakami et al., 2004; Oganov and Ono, 2004; Tsuchiya et al., 2004a) and is interesting in the present context for two reasons: its influence on the dynamics, and its ability to explain various seismological observations, starting with the much-studied shear-wave discontinuity atop D″ discovered by Lay and Helmberger (1983). This phase transition has a strongly positive Clapeyron slope, initially estimated at ~8 MPa/K (Oganov and Ono, 2004; Tsuchiya et al., 2004b), but this is probably a lower bound (Hernlund and Labrosse, 2007) and values as high as 13 MPa/K may be appropriate (Tateno et al., 2009; Hernlund, 2010).

If the CMB temperature is in the post-perovskite stability field then the perovskite-to-post-perovskite transition will exist everywhere with a variable depth depending on the local temperature profile (Fig. 11 dot-dashed line). If, however, the CMB temperature is in the perovskite stability field (Fig. 11 dotted and dashed lines) then post-perovskite will only exist in regions that have a cold-to average temperature, with a "double crossing" of the phase boundary with increasing depth (first Pv→pPv with a positive S-wave velocity (*Vs*) jump, then pPv→Pv with a negative *Vs* jump), while in hot areas it would not occur at all (Hernlund et al., 2005). From core-related constraints on the CMB temperature and mineral physics constraints on the post-perovskite phase transition parameters it is not clear which of these alternatives applies. Several seismological studies provide support for the double-crossing scenario in the sense of detecting a *Vs* increase followed by a *Vs* decrease (Thomas et al., 2004a; Thomas et al., 2004b; Hernlund et al., 2005; Avants et al., 2006; Lay et al., 2006; Kawai et al., 2007a; Kawai et al., 2007b; van der Hilst et al., 2007; Sun and Helmberger, 2008; Kawai et al., 2009; Kawai and Geller, 2010). Caution must, however, be exercised in interpreting a *Vs* decrease close to the CMB, because the expected rapid increase in

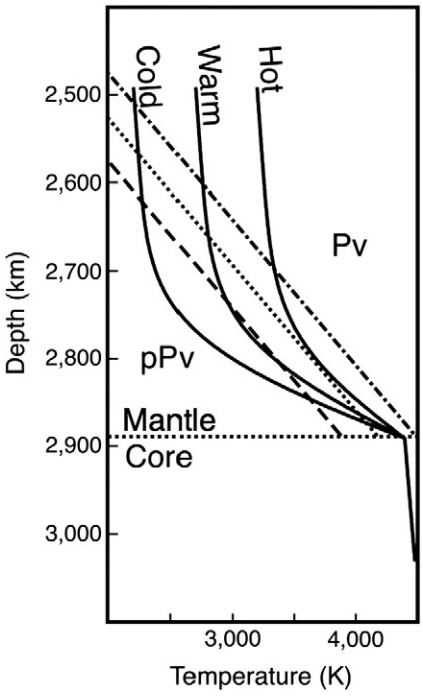

Fig. 11. Geotherms and PPV phase boundaries for three different compositions (dashed, dotted and dot-dashed lines) and three different geotherms (labelled hot, warm and cold). For material with an effective phase boundary temperature higher than the CMB temperature (dot-dashed), a single-, rather than double-, crossing is expected. Reproduced from Tackley et al. (2007).

temperature would also cause such a feature. Mineralogical and seismological constraints on post-perovskite are further reviewed in Hirose (2007) and Lay and Garnero (2007), with a broader review of deep mantle mineralogical complexities in Tronnes (2010).

4.2. Dynamical influences

4.2.1. Clapeyron slope

The dynamical influences of the post-perovskite transition come from two effects: its positive Clapeyron slope and its influence on physical properties, particularly viscosity. This positive Clapeyron slope means that hotter than average regions undergo the transition at higher pressure (depth) and colder regions at lower depth, creating lateral density anomalies that enhance convective instability, resulting in more plumes and a warmer mantle, as shown in 2-D (Nakagawa and Tackley, 2004a; Matyska and Yuen, 2005, 2006; Yuen et al., 2007) and in 3-D (Nakagawa and Tackley, 2006; Tackley et al., 2007). This is visible from a comparison of the middle and right panels of Fig. 4, which differ only in that the middle panel case contains the pPv transition. The magnitude of these effects is greatest if the pPv transition is embedded in the lower TBL rather than above it (Tackley et al., 2007). This destabilising effect is, however, relatively small despite the large Clapeyron slope, because the density contrast is small, and so it probably has less influence than other uncertainties in deep mantle parameters (such as the density of MORB). Using 3-D spherical convection simulations, Monnereau and Yuen (2007) found that the shape of the pPv surface is sensitive to amount of internal heating, Clapeyron slope and temperature at which the pPv transition intercepts the CMB, with the best match to seismic observations found when the Clapeyron slope is >9 MPa/K, a relatively high intercept temperature and 80% internal heating.

Piles of dense material tend to be hot (Fig. 7) so there is less or no post-perovskite inside them if the transition is composition-independent (Fig. 12 top panel). This results in an anti-correlation between regions of dense material and regions containing post-perovskite, which has the effect of destabilising the piles (Nakagawa and Tackley, 2005b). The sides of post-perovskite regions can be sharp and vertical, and thus may offer an alternative explanation for explaining some seismological observations (Ni et al., 2002; To et al., 2005).

Adding complexity to this picture, the pressure and sharpness of the pPv transition does depend on composition (Caracas and Cohen, 2005; Catalli et al., 2009) such that it occurs at lower pressure in MORB than in pyrolite (Ohta et al., 2008a), which is consistent with seismological observations of a post-perovskite lens in the hot, probably dense region in the central Pacific (Lay et al., 2006). Fig. 12 lower panel illustrates that when the pPv transition occurs at a lower pressure in MORB, pPv occurs everywhere but with some complexity at the edges of piles. Such composition-dependence eliminates the destabilisation effect (Tackley et al., 2007).

4.2.2. Physical properties

Post-perovskite may have different physical properties than perovskite (in addition to the obvious density difference), including thermal conductivity (Goncharov et al., 2010), electrical conductivity (Ohta et al., 2008b) and most importantly, viscosity. The mechanical properties of pPv, including seismic velocity and viscosity, are strongly anisotropic due to its crystal structure (Stackhouse et al., 2005; Wentzcovitch et al., 2006). Seismological observations of strong anisotropy at the base of the mantle combined with the expected strong LPO seismic anisotropy of post-perovskite (Yamazaki et al., 2006; Walte et al., 2007) led to the idea that post-perovskite is undergoing dislocation creep while perovskite undergoes diffusion creep. A relatively low dislocation creep viscosity was argued by Carrez et al. (2007), and a reduction in viscosity was indeed observed in analogue material $CaIrO_3$ when transforming from perovskite to pPv (Hunt et al., 2009). Based on ab initio calculations, Ammann et al. (2010) proposed that the diffusion creep viscosity is also lower than that of perovskite by as much as 2–3 orders of magnitude. This is not certain because its viscosity is highly anisotropic, varying by several orders of magnitude depending on the slip direction (Ammann et al., 2010), so it is not clear what the macroscopic effective viscosity of an assemblage of grains is. While Ammann et al. (2010) argue that the easiest slip system will dominate the overall strength, this has been questioned (Karato, 2010). Another mechanism by which viscosity could be reduced in post-perovskite is grain size reduction accompanying the phase transition, as previously discussed for other phase transitions (e.g. Karato et al., 2001; Solomatov, 2001) and observed during the transformation of $CaIrO_3$ from the perovskite to post-perovskite structure (Hunt et al., 2009).

As post-pervoskite tends to occur in cold material due to its positive Clapeyron slope, low-viscosity post-perovskite strongly influences (facilitates) slab deformation above the CMB, resulting in locally higher CMB heat flux (Cizkova et al., 2010) and in structures that resemble some seismic results (van den Berg et al., 2010). Global 3-D spherical calculations (Nakagawa and Tackley, 2011) in which the pPv viscosity is lowered by a factor of 100 show that this local weakening can also have a major effect on global heat flux and convective velocities, and that it also influences the morphology of dense 'piles' because the slab material is able to spread more effectively, and because a larger amount of MORB settles at the CMB.

There is some evidence for low-viscosity post-perovskite from the geoid. Instantaneous flow calculations designed to model the geoid indicate that including low viscosity in regions where post-perovskite is expected to be present improves the global fit to Earth's geoid (Cadek and Fleitout, 2006). This is because low-viscosity pPv changes the flow pattern near the CMB, decreasing the geoid above slabs (Tosi et al., 2009a; Tosi et al., 2009b).

4.3. Seismic structure

Post-perovskite has a strong influence on seismic structure and heterogeneity in the deep mantle. It is the most likely explanation for the discontinuity in S-wave velocities that occurs at different heights above the CMB and is observed in some areas but not others (Lay and Helmberger, 1983; Young and Lay, 1987, 1990; Gaherty and Lay, 1992; Ding and Helmberger, 1997; Wysession et al., 1998; Sun and Helmberger, 2008), as argued presciently by Sidorin et al. (1999a,b). In contrast, the P-wave and bulk sound velocities are slightly lower (Wookey et al., 2005; Shim et al., 2008). Detailed analysis of deep mantle structure under the Cocos plate (Hutko et al., 2008) finds a strong S-wave velocity increase accompanied by a weak decrease in P-wave velocity, exactly as expected for pPv (Wookey et al., 2005; Hustoft et al., 2008). Post-perovskite may provide an explanation for Vs–Vp decorrelation in the deepest ~200 km of the mantle, although not above that (Hernlund and Houser, 2008). As discussed earlier, pPv may actually generate two discontinuities (Hernlund et al., 2005), for which several seismic studies provide evidence. A detailed review of seismological imaging of the deep mantle is (Lay and Garnero, 2011).

The presence of impurities such as aluminium cause the pPv transition to be more spread out in pressure space (Akber-Knutson et al., 2005), such that for a pyrolitic composition it might be 100 s km thick (Catalli et al., 2009), which would be seismically undetectable. However, consideration of the detailed temperature structure including latent heat effects indicates that the transition can appear seismically sharp even if the phase loop is fairly broad (Hernlund, 2010). Differences in composition also affect the depth of the transition, such that it occurs at lower pressure in MORB than in pyrolite (Ohta et al., 2008a), which is consistent with seismological observations of a post-perovskite lens in the hot, probably dense region in the central Pacific (Lay et al., 2006).

The S-wave velocity contrast caused by the pPv transition is quite large at 1–2% — of the same order as the total velocity contrasts due to temperature or composition, and therefore lateral variability in the occurrence of post-perovskite causes strong seismic heterogeneity in the

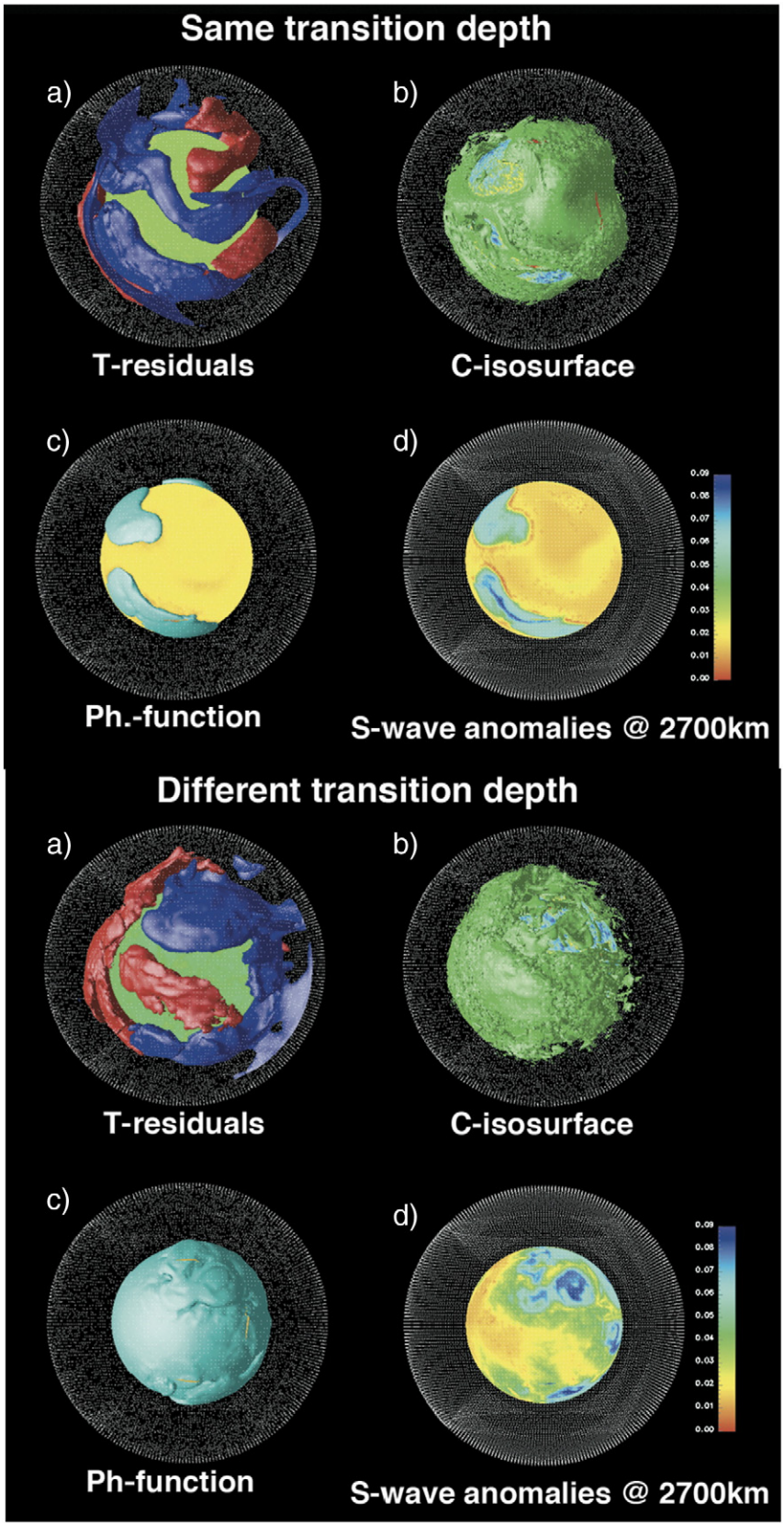

Fig. 12. Thermo-chemical convection in 3D spherical geometry, showing the effects of composition-independent pPv phase transition depth (top panel) compared to composition-dependent pPv depth (bottom panel). In each panel the plots are: (a) Residual temperature isosurfaces showing where the temperature is 250 K higher (red) or 250 K lower (blue) than the geotherm, with the upper 400 km removed to expose the deep mantle. (b) Compositional isosurface showing 75% MORB, again with the upper 400 km removed. (c) Location of at least 50% volume fraction post-perovskite. (d) S-wave anomalies at 2700 km depth, where Vs varies by 2% both for composition and with PPV.
Reproduced from Tackley et al. (2007).

deepest mantle. Synthetic seismic spectra at 2700 km depth (Nakagawa and Tackley, 2006) or plotted as a function of radius (Tackley et al., 2007) indicate that post-perovskite may be the dominant contribution to globally-averaged (spherical harmonic) seismic heterogeneity in the deepest part of the mantle, and has a different spectrum to the heterogeneity caused by thermal or compositional variations. It also leads to sharp vertical structures, which may explain some seismological observations.

As mentioned in Section 4.2.2 pPv is strongly anisotropic. If the crystals are aligned by deformation (which occurs during dislocation creep), then this will cause lattice preferred orientation (LPO) anisotropy in regions where pPv is deformed in the deep mantle (Yamazaki et al., 2006). The alternative mechanism for generating anisotropy is shape preferred orientation (SPO) of heterogeneous materials such as inclusions and melt. An early attempt to simulate anisotropy development by flow in a pPv D″ layer (Merkel et al., 2007) found that it is difficult to reproduce seismically-observed anisotropy using this mechanism. Miyagi et al. (2010), however, found that slip probably occurs on a different system than previously assumed, producing a pattern of anisotropy that is consistent with seismic observations. Assuming this new slip system, Wenk et al. (2011) calculated anisotropy development in a convection cell that included a slab reaching the CMB and the development of plumes, finding that it indeed looks like observed seismic anisotropy. Consistent with early calculations of deformation during convection (McKenzie, 1979) the long strain direction close to the boundary aligns with the flow.

4.4. Estimating CMB heat flux

By combining the seismologically-inferred position of the pPv phase transition with information about the Clapeyron slope of the transition, it is possible to place a bound on the local temperature gradient in the region of observation, and by combining this with an estimate of thermal conductivity, obtain the local CMB heat flux. In particular, if a double-crossing is observed then the temperature gradient with pressure must be at least the inverse of the Clapeyron slope. A problem with this approach is that, as discussed in Section 2.3, estimates of the deep mantle thermal conductivity vary by a factor of ~4.5. Application of this technique assuming a thermal conductivity of 10 W/m-K has yielded local CMB heat flux estimates of 60–80 mW/m^2 under Eurasia and the Caribbean (Hernlund et al., 2005), 85 ± 25 mW/m^2 underneath the central Pacific (Lay et al., 2006) and 115 ± 45 mW/m^2 under Central and North America (van der Hilst et al., 2007). Areas where post-perovskite is present tend, however, to be colder than average areas, which, according to global convection models (Nakagawa and Tackley, 2008) may have local heat flux as much as a factor of two higher than the global average. Another complication is that the temperature profile above the CMB is not linear or error function. Buffett (2007) showed that if the pPv transition drives downwards flow then the heat flux can be much higher. Using 3-D spherical convection calculations, Monnereau and Yuen (2007, 2010) studied the relationship between seismic structure (depth of phase transition crossings) and local heat flux, finding a more complex relationship than linear, with the exact relationship depending on the profiles of viscosity and thermal conductivity. They concluded that a range of CMB heat flux of 5–17 TW are consistent with seismic observations, depending on the deep mantle thermal conductivity.

5. Ultra-low Velocity Zones (ULVZs)

5.1. Background

A number of geographically localised and vertically thin (~10 s km) zones of very low (5–10% lower than average) seismic velocity directly above the CMB have been detected since the mid-1990s (Garnero and Helmberger, 1995, 1996). These have commonly been interpreted as being due to the presence of 10–30% partial melt (Williams and Garnero, 1996; Revenaugh and Meyer, 1997; Vidale and Hedlin, 1998; Wen and Helmberger, 1998; Garnero, 2004), although some type of iron-enriched solid could also explain the seismic signature, either forming in the mantle, as discussed below, or by accumulated silicate sediments from the core (Buffett et al., 2000). The mantle-side explanations are reviewed in detail in the next two sections.

The locations of detected ULVZs are not random, but rather are statistically correlated with hotspot locations (Williams et al., 1998), and also the edges of large, seismically-slow regions (McNamara et al., 2010) that are commonly inferred to be compositionally-distinct, as discussed in Section 3.

5.2. Partial melt?

Partial melting requires that the CMB temperature be higher than the solidus temperature at that pressure. This is plausible but highly uncertain. Estimates of the solidus for pyrolite come from melting experiments or ab initio calculations, with recent determinations for the value at CMB pressure being quite consistent: 4100 K (Stixrude et al., 2009), 4180 ± 150 K (Fiquet et al., 2010) and 4150 ± 150 K (Andrault et al., 2011), which are also consistent with the upper bound of 4300 K found earlier by Zerr et al. (1998). Estimates of the CMB temperature, discussed in Section 2.1, come from consideration of the core phase diagram and are highly uncertain, but commonly-quoted values are in the range 3700–4300 K (Boehler, 2000; Price et al., 2004).

Because the CMB is very close to being isothermal, partial melt should exist everywhere at the CMB with a variable thickness depending on the local temperature gradient. An exception to this would be if compositional variations exist at the CMB and different compositions have different solidus temperatures; in particular, MORB probably has lower solidus than pyrolite (Ohtani and Maeda, 2001; Stixrude et al., 2009). Because ULVZs are not observed in some areas (e.g. Rost et al., 2010a,b), it therefore appears that they must be compositionally distinct and probably iron enriched.

If ULVZs are caused by a fairly large fraction of partial melt, then why does the melt stay in the solid matrix and not drain out into a pure melt layer above the CMB (if it is denser than the solid) or rise into the colder mantle above and solidify (if it is buoyant)? Dynamical calculations of the deepest mantle including two-phase flow indicated a very narrow parameter range, in which the melt is very slightly denser than solid and the permeability is curiously very low, under which melt would remain in the solid to form ULVZ-like features (Hernlund and Tackley, 2007). These calculations, however, used a simplified treatment of melt migration in which the driving force for melt percolation was purely gravity acting on the density difference between solid and liquid. Hernlund and Jellinek (2010) showed that when dynamic pressure gradients associated with deformation of the solid matrix by surrounding flow are also included, dynamic pressure gradients can dominate gravitational settling and allow the melt to stay in suspension in the solid.

A melt explanation for ULVZs thus requires the melt to be slightly denser than the solid at deep mantle pressures, so a key question is whether this is the case. There is increasing evidence that it is. Extrapolations of laboratory data (Agee, 1998; Ohtani and Maeda, 2001) indicate that basaltic melt becomes denser than solid peridotite, although peridotitic melt does not. Shock-wave experiments (Akins et al., 2004; Mosenfelder et al., 2007; Mosenfelder et al., 2009) indicate that melt may indeed be slightly denser than perovskite, although less dense than post-perovskite (Mosenfelder et al., 2009). Molecular dynamics simulations (Stixrude et al., 2009) indicate that although $MgSiO_3$ melt is slightly less dense than the solid counterpart at CMB pressures, if Fe partitioning is considered then the melt could be more dense. This is reinforced by the laboratory experiments of (Nomura et al., 2011), who find that both systematic changes in Fe and (Fe + Mg) partitioning with pressure, and the iron spin transition, combine to make melt denser in the lower ~1000 km of the mantle.

If the base of the mantle is partially molten today, it is obvious that a larger volume of it would have been molten in the past when the mantle and core were hotter (e.g. Sharpe and Peltier, 1978). Labrosse et al. (2007) termed this partially molten region at the base of the mantle the 'basal magma ocean' (BMO), and outlined how it would have influenced the thermo-chemical evolution of the Earth. If the mantle was entirely molten after the moon-forming impact, as is commonly believed, then it would have solidified from the middle rather than bottom as was previously thought (Solomatov, 2007). This scenario is supported by subsequent studies (Mosenfelder et al., 2009; Stixrude et al., 2009). Other consequences are that as the BMO crystallised over Earth's history, the composition of the remaining liquid would have changed to more Fe rich, as would the composition of the crystallising solid. Incompatible trace elements, such as those producing heat, would tend to be concentrated in the remaining liquid (Corgne et al., 2005). A layer of liquid around the core would have suppressed lateral variations in CMB heat flux. Eventually the BMO would completely solidify, with the last-forming solids being highly iron-enriched, which might be a better match for ULVZ observations than partial melt (Nomura et al., 2011).

5.3. Fe-enriched solid?

Various solid compositions are also plausible candidates for explaining seismic ULVZ observations, and may even match better than partial melt. The properties of iron-rich post-perovskite, whether ferrous (Caracas and Cohen, 2005; Mao et al., 2006; Stackhouse et al., 2006) or ferric (Stackhouse and Brodholt, 2008) could also explain the seismic velocities. Recent results indicate another possible solid composition: a mixture of iron-enriched (Mg,Fe)O magnesiowüstite and ambient mantle (Wicks et al., 2010; Bower et al., 2011).

If ULVZs are iron-enriched solid, where did this material come from? Three possibilities have been proposed:

(i) Subducted banded-iron formations were proposed as the origin of ULVZs by Dobson and Brodholt (2005).
(ii) Progressive crystallisation of a basal magma ocean (BMO) above the CMB (Labrosse et al., 2007) would result in an increasingly Fe-enriched liquid, which would eventually solidify to form an Fe-enriched solid (Nomura et al., 2011) that might match ULVZ properties.
(iii) Chemical reactions with the core have received much attention (Knittle and Jeanloz, 1991; Song and Ahrens, 1994; Dubrovinsky et al., 2001; Dubrovinsky et al., 2003). Such chemical reactions would be expected to occur over rather small length scales making it difficult to build up a significant layer: a penetration by liquid Fe of 1–100 m was estimated by Poirier (1993) and Poirier and Le Mouel (1992). A much more efficient mechanism is a suction in areas of downwelling (where the CMB is depressed), which may entrain Fe a distance ~1 km into the mantle with fractions of up to 10% (Kanda and Stevenson, 2006). Another dynamical mechanism for enhancing Fe transfer is shear-aided dilatency in regions that already contain a substantial silicate melt fraction: above a critical strain rate of order (10^{-12} s^{-1}) significant amounts of liquid Fe can percolate upwards into the silicate matrix (Petford et al., 2005; Petford et al., 2007). For either mechanism it remains to be determined whether at these reaction rates, a sufficient amount of Fe-rich material to explain ULVZs can build up over geological time.

The dynamical feasibility of the 'dense solid' explanation was demonstrated by McNamara et al. (2010) using calculations of thermo-chemical convection with two types of dense material, one representing piles and one with the density seismically-inferred for ULVZs. They showed that small volumes of solid ULVZ material can be locally elevated despite its high density, and are swept around by the convection to the boundaries of large compositional accumulations, which periodically break apart and merge together in response to changes in downwelling patterns.

If ULVZs are enriched in iron, then they could have substantially higher thermal conductivity (Manga and Jeanloz, 1996), which would influence their temperature profiles, although they are small enough that this might not have a major effect on large-scale flow.

6. Synthesis

The last decade has seen an astonishing improvement in our knowledge of the deep mantle due to improvements in seismological data and techniques for mapping both large- and small-scale structure, mineral physics (particularly the discovery of post-perovskite and the iron spin transition, but also physical properties such as those of melts) and dynamical modelling, such that views of the present-day structure of the deep mantle seem to be converging towards a consensus. Components of this consensus include two large-scale thermo-chemical dense piles underneath the Pacific and Africa with a total volume of approximately a few percent of the mantle volume (Section 3.3.2; Fig. 9), shear-wave velocity discontinuities caused by the perovskite to post-perovskite transition (Sections 4.1, 4.3), scattered pockets of dense, iron-enriched solid or partial melt that get swept to the edges of the piles (Section 4.3), a tendency for plumes to arise from the edges of these piles (Section 3.5), and strong anisotropy aligned with the local flow direction in D″ (Section 4.3). The field has reached the stage where individual 'blobs' in seismic tomographic models can be identified as features from historical plate reconstructions (van der Meer et al., 2010). It is thus easy to get the impression that all that is left to do is work out a few details and write review papers (e.g. Garnero and McNamara, 2008; Tronnes, 2010).

Even if deep mantle structure were known in minute detail, however, fundamental questions would still remain — in particular, how the deep mantle developed its present structure as a result of 4.5 billion years of evolution. This encompasses many individual questions, including: What is the dense material and how did it get there? How can geochemical observations be reconciled with geophysically-inferred structures? Are ULVZs solid or partially molten? How are deep mantle processes linked to geological observations? Furthermore, large uncertainties in various deep mantle physical properties discussed earlier, including the dependence of viscosity on various factors, the thermal conductivity, phase relationships, elemental partitioning and melting in the deep mantle taking into account post-perovskite, iron spin transitions, etc., preclude a precise quantitative understanding at this stage.

The origin of dense material in the deep mantle is of particular interest; various primordial or recycled possible origins were discussed in Section 3.2. Most likely it does not have a single origin but is a mélange of various things, as shown in Fig. 13. Melting is the dominant process in its creation. After the moon-forming impact the Earth was likely completely molten, and according to recent data the mantle would have solidified from the middle with the deepest ~800–1000 km of the mantle containing a basal magma ocean that became increasingly iron-rich as the mantle progressively crystallised (Labrosse et al., 2007; Stixrude et al., 2009; Nomura et al., 2011), although there is still some uncertainty about this scenario (Andrault et al., 2011). Widespread melting in the upper mantle would have created negatively-buoyant melts and subsequently dense solids that could have sunk to the deepest mantle, so-called upside-down differentiation (Lee et al., 2010), joining the partially-molten material that was already there. Extensive early crust would also have been generated due to widespread melting, and this might also have subducted and sunk into the deepest mantle (Boyet and Carlson, 2005; Tolstikhin and Hofmann, 2005; Tolstikhin et al., 2006). Subsequently, over billions of years, large volumes of subducted oceanic crust, and possibly some smaller amount of continental crust (Komabayashi et al., 2009; Senshu

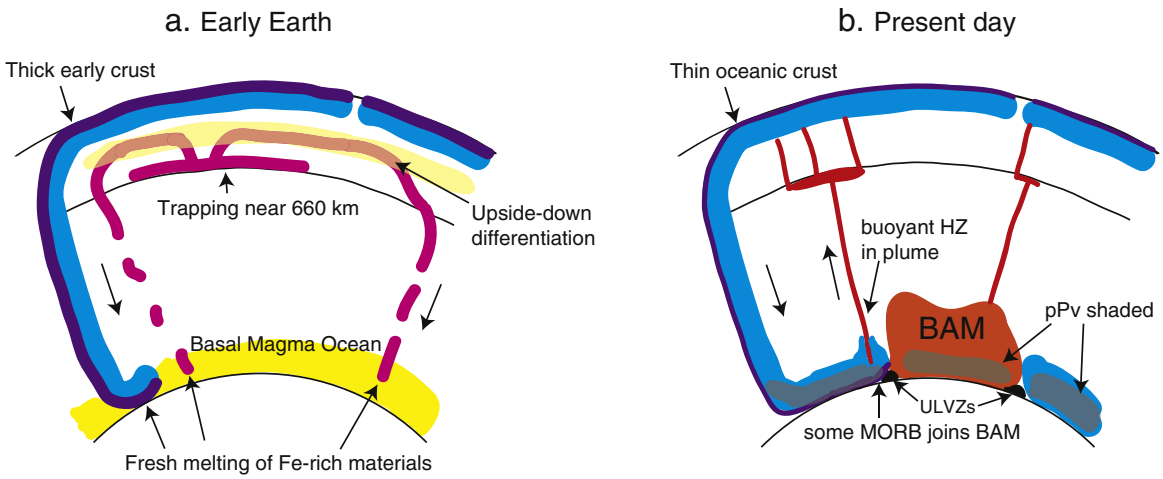

Fig. 13. Plausible scenario of deep mantle processes in (a) the early Earth and (b) present day. In the early Earth, iron-rich materials from several sources including basal magma ocean (Labrosse et al., 2007), upside-down differentiation (Lee et al., 2010) and overturn of early crust (Tolstikhin et al., 2006) accumulated in the deep mantle generating the basal mélange (BAM). At the present day, BAM exists in two large piles and the remains of the basal magma ocean are in ULVZs. For a full discussion see text.

et al., 2009) would have also reached this region and become assimilated to some extent (Fig. 13b).

The result of these combined early and ongoing processes is a heterogeneous basal mélange (BAM). All of these materials would be enriched in iron and incompatible trace elements, although their detailed compositions would vary due to different formation pressures and melt fractions. Melting in the deepest mantle likely existed over much of Earth history (Labrosse et al., 2007) and would have served to mix and equilibrate these incoming materials to some extent, as incoming iron-rich material that reached existing hot melt would have melted itself (Fig. 13a). It is also possible that different materials retained some of their original chemical identity, particularly the deep mantle became mostly solid. The last remaining pockets of partial melt would be highly concentrated in iron and could explain ULVZs, possibly after solidifying (Nomura et al., 2011).

Geochemical observations are typically interpreted to require a need for storage of three main types of material (Hofmann, 1997): (i) with a primitive noble gas signature (i.e., that has never degassed), (ii) containing incompatible trace elements that are 'missing' from the sampled mantle according to Earth composition models, and (iii) recycled material, with oceanic crust producing the HIMU end-member and continental material producing the EM1 and EM2 end-members (Stracke et al., 2005; Willbold and Stracke, 2006). There has been much debate about these interpretations and some alternative concepts (e.g. reviewed in Tackley (2007)) that will not be discussed here; briefly, recycled crust can offer an explanation for (ii) and (iii) (e.g. Coltice et al., 2000), while melt products that formed at greater depth and therefore never degassed could explain (i) and (ii). Therefore, BAM has the potential to explain the various geochemical observations.

Given the enormous amount of iron-enriched material that has probably formed in or reached the deep mantle over geological time, it is perhaps surprising that the volume of BAM is not a great deal larger than inferred from seismic observations: for example Hernlund and Houser (2008) estimate a volume of only 2% of the mantle volume. On the other hand, simulations of pile formation by segregation of subducted MORB find that 2% is a reasonable equilibrium volume at an Earth-like convective vigour (Christensen and Hofmann, 1994; Brandenburg and van Keken, 2007). Therefore, a plausible scenario for the evolution of the BAM is that it was very large early on due to the basal magma ocean and subsequent rapid arrival of other material, but has decreased in size over time to its present equilibrium value. Entrainment is also more rapid at higher Rayleigh number (Eq. 4), which would have characterised the early Earth, so the volume could have decreased quite rapidly as heterogeneities got rapidly remixed (Coltice et al., 2009; Caro, 2011). A complicating factor is that phase transitions around 660 km depth have a much higher influence at higher Ra, both for thermal convection (Christensen and Yuen, 1985) and thermo-chemical convection (Davies, 2008), which might have caused significant flow layering early on, reducing the rate of entrainment (Deschamps and Tackley, 2009).

According to inferences that present-day plumes and the reconstructed locations of erupting LIPs both come from the edges of BAM piles, these piles have remained in a similar position for the last few 100 s Ma (Burke and Torsvik, 2004; Thorne et al., 2004; Torsvik et al., 2006; Burke et al., 2008; Torsvik et al., 2008), and there has even been a proposal that the large-scale structure of the deep mantle has been stable for billions of years (Dziewonski et al., 2010). In all laboratory or numerical experiments of thermo-chemical convection in which the flow is time-dependent, however, piles are swept around by the large-scale flow and sometimes split by new downwelling slabs (e.g., Figs. 7 and 10 here and Davaille et al., 2002; Hansen and Yuen, 1989; McNamara et al., 2010; Tan et al., 2011). Convection models in which supercontinent aggregation is included demonstrate a supercontinent's ability to reorganise and even reverse the long-wavelength flow (e.g. Grigne et al., 2007; Gurnis, 1988; Honda et al., 2000; Lowman and Jarvis, 1993). Thus, stability for billions of years seems unlikely. Even in time-dependent, chaotic convection, however, there are sometimes features that remain in a similar position for some time; for example the pile near the bottom of the simulation in Fig. 7. Thus, a special explanation for approximately few 100 s Ma fixity of BAM piles is probably not required. It has been proposed, based on geological observations, that broad upwelling "superplumes" rising from these BAM piles have played a major role in Earth's mantle evolution (Maruyama, 1994; Maruyama et al., 2007).

Future progress in understanding the deep mantle will require advanced modelling to understand present-day structure in the context of long-term evolution, which will in turn require better knowledge of the relevant mineral physics properties. Seismological observations of increasing resolution will continue to play a key role in unravelling present-day structures.

Acknowledgements

This invited review paper resulted from an invited review talk at the 2010 SEDI conference at UC Santa Barbara. The author thanks the organisers of that conference. The author thanks David Yuen and Thorne Lay for constructive reviews.

References

Abe, Y., 1997. Thermal and chemical evolution of the terrestrial magma ocean. Physics of the Earth and Planetary Interiors 100, 27–39.

Agee, C.B., 1998. Crystal-liquid density inversions in terrestrial and lunar magmas. Physics of the Earth and Planetary Interiors 107, 63–74.

Akaogi, M., Ito, E., 1993. Refinement of enthalpy measurement of $MgSiO_3$ perovskite and negative pressure-temperature slopes for perovskite-forming reactions. Geophysical Research Letters 20, 1839–1842.

Akber-Knutson, S., Steinle-Neumann, G., Asimow, P.D., 2005. Effect of Al on the sharpness of the MgSiO3 perovskite to post-perovskite phase transition. Geophysical Research Letters 32, L14303 doi:14310.11029/12005gl023192.

Akins, J.A., Luo, S.-N., Asimow, P.D., Ahrens, T.J., 2004. Shock-induced melting of MgSiO3 perovskite and implications for melts in Earth's lowermost mantle. Geophysical Research Letters 31, L14612 doi:14610.11029/12004gl020237.

Amit, H., Choblet, G., 2010. Mantle-driven geodynamo features — effects of post-Perovskite phase transition. Earth and Planetary Space 61, 1255–1268.

Ammann, M.W., Brodholt, J.P., Dobson, D.P., 2009. DFT study of migration enthalpies in MgSiO3 perovskite. Physics and Chemistry of Minerals 36, 151–158. doi:10.1007/s00269-00008-00265-z.

Ammann, M.W., Brodholt, J.P., Wookey, J., Dobson, D.P., 2010. First-principles constraints on diffusion in lower-mantle minerals and a weak D″ layer. Nature 465, 462–465.

Ammann, M.W., Brodholt, J.P., Dobson, D.P., 2011. Ferrous iron diffusion in ferro-periclase across the spin transition. Earth and Planetary Science Letters 302, 393–402.

Anderson, D.L., 1987. A seismic equation of state.2. Shear properties and thermodynamics of the lower mantle. Physics of the Earth and Planetary Interiors 45, 307–323.

Anderson, O.L., Oda, H., Isaak, D., 1992. A model for the computation of thermal expansivity at high compression and high temperatures — MgO as an example. Geophysical Research Letters 19, 1987–1990.

Andrault, D., Bolfan-Casanova, N., Nigro, G.L., Bouhifd, M.A., Garbarino, G., Mezouar, M., 2011. Solidus and liquidus profiles of chondritic mantle: implication for melting of the Earth across its history. Earth and Planetary Science Letters 304, 251–259.

Antolik, M., Gu, Y.J., Ekstrom, G., Dziewonski, A.M., 2003. J362D28: a new joint model of compressional and shear velocity in the Earth's mantle. Geophysical Journal International 153, 443–466.

Asanuma, H., Ohtani, E., Sakai, T., Terasaki, H., Kamada, S., Kondo, T., Kikegawa, T., 2010. Melting of iron–silicon alloy up to the core–mantle boundary pressure: implications to the thermal structure of the Earth's core. Physics and Chemistry of Minerals 37, 353–359 (359).

Aubert, J., Amit, H., Hulot, G., Olson, P., 2008. Thermochemical flows couple the Earth's inner core growth to mantle heterogeneity. Nature 454, 758–761.

Avants, M., Lay, T., Russell, S.A., Garnero, E.J., 2006. Shear velocity variation within the D ″ region beneath the central Pacific. Journal of Geophysical Research 111, B05305 doi:05310.01029/02004JB003270.

Badro, J., Fiquet, G., Guyot, F., Rueff, J.-P., Struzhkin, V.V., Vanko, G., Monaco, G., 2003. Iron partitioning in Earth's mantle: toward a deep lower mantle discontinuity. Science 300, 789–791.

Badro, J., Rueff, J.P., Vanko, G., Monaco, G., Fiquet, G., Guyot, F., 2004. Electronic transitions in perovskite: possible nonconvecting layers in the lower mantle. Science 305, 383–386.

Balachandar, S., Yuen, D.A., Reuteler, D., 1992. Time-dependent 3-dimensional compressible convection with depth-dependent properties. Geophysical Research Letters 19, 2247–2250.

Becker, T.W., Boschi, L., 2002. A comparison of tomographic and geodynamic mantle models. Geochemistry, Geophysics, Geosystems 3 (Paper number 2001GC000168).

Becker, T.W., Kellogg, J.B., O'Connell, R.J., 1999. Thermal constraints on the survival of primitive blobs in the lower mantle. Earth and Planetary Science Letters 171, 351–365.

Bercovici, D., Schubert, G., Glatzmaier, G.A., 1989. Influence of heating mode on 3-dimensional mantle convection. Geophysical Research Letters 16, 617–620.

Boehler, R., 2000. High-pressure experiments and the phase diagram of lower mantle and core materials. Reviews of Geophysics 38, 221–245.

Bower, D.J., Wicks, J.K., Gurnis, M., Jackson, J.M., 2011. A geodynamic and mineral physics model of a solid-state ultralow-velocity zone. Earth and Planetary Science Letters 303, 193–202.

Boyet, M., Carlson, R.W., 2005. ^{142}Nd evidence for early (>4.53 Ga) global differentiation of the silicate Earth. Science 309, 576–581.

Brandenburg, J.P., van Keken, P.E., 2007. Deep storage of oceanic crust in a vigorously convecting mantle. Journal of Geophysical Research 112. doi:10.1029/2006JB004813.

Brandenburg, J.P., Hauri, E.H., van Keken, P.E., Ballentine, C.J., 2008. A multiple-system study of the geochemical evolution of the mantle with force-balanced plates and thermochemical effects. Earth and Planetary Science Letters 276, 1–13.

Brown, J.M., Shankland, T.J., 1981. Thermodynamic parameters in the Earth as determined from seismic profiles. Geophysical Journal of the Royal Astronomical Society 66, 579–596.

Buffett, B.A., 2002. Estimates of heat flow in the deep mantle based on the power requirements for the geodynamo. Geophysical Research Letters 29. doi:10.1029/2001GL014649.

Buffett, B.A., 2007. A bound on heat flow below a double crossing of the perovskite–postperovskite phase transition. Geophysical Research Letters 34. doi:10.1029/2007GL030930.

Buffett, B.A., Garnero, E.J., Jeanloz, R., 2000. Sediments at the top of Earth's core. Science 290, 1338–1342.

Bull, A.L., McNamara, A.K., Ritsema, J., 2009. Synthetic tomography of plume clusters and thermochemical piles. Earth and Planetary Science Letters 278, 152–162.

Bunge, H.-P., 2005. Low plume excess temperature and high core heat flux inferred from non-adiabatic geotherms in internally heated mantle circulation models. Physics of the Earth and Planetary Interiors 153, 3–10.

Bunge, H.P., Richards, M.A., Baumgardner, J.R., 1996. Effect of depth-dependent viscosity on the planform of mantle convection. Nature 379, 436–438.

Burke, K., Torsvik, T.H., 2004. Derivation of Large Igneous Provinces of the past 200 million years from long-term heterogeneities in the deep mantle. Earth and Planetary Science Letters 227, 531–538.

Burke, K., Steinberger, B., Torsvik, T.H., Smethurst, M.A., 2008. Plume generation zones at the margins of Large Low Shear Velocity Provinces on the core–mantle boundary. Earth and Planetary Science Letters 265, 49–60.

Butler, S.L., Peltier, W.R., Costin, S.O., 2005. Numerical models of the Earth's thermal history: effects of inner-core solidification and core potassium. Physics of the Earth and Planetary Interiors 152, 22–42.

Cadek, O., Fleitout, L., 2006. Effect of lateral viscosity variations in the core–mantle boundary region on predictions of the long-wavelength geoid. Studia Geophysica et Geodaetica 50, 217–232.

Campbell, I.H., Griffiths, R.W., 1990. Implications of mantle plume structure for the evolution of flood basalts. Earth and Planetary Science Letters 99, 79–93.

Caracas, R., Cohen, R.E., 2005. Effect of chemistry on the stability and elasticity of the perovskite and post-perovskite phases in the $MgSiO_3$–$FeSiO_3$–Al_2O_3 system and implications for the lowermost mantle. Geophysical Research Letters 32, L16310 doi:16310.11029/12005gl023164.

Caro, G., 2011. Early silicate Earth differentiation. Annual Review of Earth and Planetary Sciences 39, 31–58.

Carrez, P., Ferre, D., Cordier, P., 2007. Implications for plastic flow in the deep mantle from modelling dislocations in $MgSiO_3$ minerals. Nature 446, 68–70.

Catalli, K., Shim, S.-H., Prakapenka, V., 2009. Thickness and Clapeyron slope of the post-perovskite boundary. Nature 462, 782–786.

Chopelas, A., Boehler, R., 1992. Thermal expansivity in the lower mantle. Geophysical Research Letters 19, 1983–1986.

Christensen, U., 1984. Instability of a hot boundary layer and initiation of thermochemical plumes. Annals of Geophysics 2, 311–319.

Christensen, U.R., 1989. Models of mantle convection — one or several layers. Philosophical Transactions of the Royal Society of London 328, 417–424.

Christensen, U.R., Hofmann, A.W., 1994. Segregation of subducted oceanic crust in the convecting mantle. Journal of Geophysical Research 99, 19867–19884.

Christensen, U.R., Yuen, D.A., 1985. Layered convection induced by phase transitions. Journal of Geophysical Research 90, 10291–10300.

Cizkova, H., Cadek, O., Matyska, C., Yuen, D.A., 2010. Implications of post-perovskite transport properties for core–mantle dynamics. Physics of the Earth and Planetary Interiors 180, 235–243.

Cobden, L., Goes, S., Ravenna, M., Styles, E., Cammarano, F., Gallagher, K., Connolly, J.A.D., 2009. Thermochemical interpretation of 1-D seismic data for the lower mantle: the significance of nonadiabatic thermal gradients and compositional heterogeneity. Journal of Geophysical Research 114, B11309 doi:11310.11029/12008jb006262.

Coltice, N., Ferrachat, S., Ricard, Y., 2000. Box modeling the chemical evolution of geophysical systems: case study of the Earth's mantle. Geophysical Research Letters 27, 1579–1582.

Coltice, N., Marty, B., Yokochi, R., 2009. Xenon isotope constraints on the thermal evolution of the early Earth. Chemical Geology 266, 4–9.

Corgne, A., Liebske, C., Wood, B.J., Rubie, D.C., Frost, D.J., 2005. Silicate perovskite-melt partitioning of trace elements and geochemical signature of a deep perovskitic reservoir. Geochimica et Cosmochimica Acta 69, 485–496.

Costin, S.O., Butler, S.L., 2006. Modelling the effects of internal heating in the core and lowermost mantle on the Earth's magnetic history. Physics of the Earth and Planetary Interiors 157, 55–71.

Cserepes, L., 1993. Effect of depth-dependent viscosity on the pattern of mantle convection. Geophysical Research Letters 20, 2091–2094.

Davaille, A., 1999a. Simultaneous generation of hotspots and superswells by convection in a heterogeneous planetary mantle. Nature 402, 756–760.

Davaille, A., 1999b. Two-layer thermal convection in miscible viscous fluids. Journal of Fluid Mechanics 379, 223–253.

Davaille, A., Girard, F., Le, B.M., 2002. How to anchor hotspots in a convecting mantle? Earth and Planetary Science Letters 203, 621–634.

Davies, G.F., 1980. Thermal histories of convective Earth models and constraints on radiogenic heat production in the Earth. Journal of Geophysical Research 85, 2517–2530.

Davies, G.F., 1984. Geophysical and isotopic constraints on mantle convection — an interim synthesis. Journal of Geophysical Research 89, 6017–6040.

Davies, G.F., 1988. Ocean bathymetry and mantle convection.1. Large-scale flow and hotspots. Journal of Geophysical Research 93, 10467–10480.

Davies, G.F., 2002. Stirring geochemistry in mantle convection models with stiff plates and slabs. Geochimica et Cosmochimica Acta 66, 3125–3142.

Davies, G.F., 2008. Episodic layering of the early mantle by the 'basalt barrier' mechanism. Earth and Planetary Science Letters 275, 382–392.

de Koker, N., 2010. Thermal conductivity of MgO at high pressure: implications for the D″ region. Earth and Planetary Science Letters 292, 392–398.

Della Morra, S., Boschi, L., Tackley, P.J., Nakagawa, T., Giardini, D., 2011. Low seismic resolution cannot explain S/P decorrelation in the lower mantle. Geophysical Research Letters 38, L12303 doi:12310.11029/12011GL047559.

Deschamps, F., Tackley, P.J., 2008. Searching for models of thermo-chemical convection that explain probabilistic tomography I. Principles and influence of rheological parameters. Physics of the Earth and Planetary Interiors 171, 357–373.

Deschamps, F., Tackley, P.J., 2009. Searching for models of thermo-chemical convection that explain probabilistic tomography II — influence of physical and compositional parameters. Physics of the Earth and Planetary Interiors 176, 1–18.

Deschamps, F., Trampert, J., Tackley, P.J., 2007. Thermo-chemical structure of the lower mantle: seismological evidence and consequences for geodynamics. In: Yuen, D.A., Maruyama, S., Karato, S.I., Windley, B.F. (Eds.), Superplume: Beyond Plate Tectonics. Springer, pp. 293–320.
Ding, X., Helmberger, D.V., 1997. Modelling D″ structure beneath Central America with broadband seismic data. Physics of the Earth and Planetary Interiors 101, 245–270.
Dobson, D.P., Brodholt, J.P., 2005. Subducted banded iron formations as a source of ultralow-velocity zones at the core–mantle boundary. Nature 434, 371–374.
du Vignaux, N.M., Fleitout, L., 2001. Stretching and mixing of viscous blobs in Earth's mantle. Journal of Geophysical Research-Solid Earth 106, 30893–30908.
Dubrovinsky, L., Lin, J.-F., 2009. Mineral physics quest to the Earth's core. EOS. Transactions of the American Geophysical Union 90, 21–22.
Dubrovinsky, L., Annersten, H., Dubrovinskaia, N., Westman, F., Harryson, H., Fabrichnaya, O., Carlson, S., 2001. Chemical interaction of Fe and Al_2O_3 as a source of heteroeneity at the Earth's core–mantle boundary. Nature 412, 527–529.
Dubrovinsky, L., Dubrovinskaia, N., Langenhorst, F., Dobson, D., Rubie, D., Gessmann, C., Abrikosov, I.A., Johansson, B., Baykov, V.I., Vitos, L., Le, B.T., Crichton, W.A., Dmitriev, V., Weber, H.P., 2003. Iron-silica interaction at extreme conditions and the electrically conducting layer at the base of Earth's mantle. Nature 421, 58–61.
Dziewonski, A.M., Anderson, D.L., 1981. Preliminary reference Earth model. Physics of the Earth and Planetary Interiors 25, 297–356.
Dziewonski, A.M., Lekic, V., Romanowicz, B.A., 2010. Mantle anchor structure: an argument for bottom up tectonics. Earth and Planetary Science Letters 299, 69–79.
Farnetani, C.G., 1997. Excess temperature of mantle plumes — the role of chemical stratification across D″. Geophysical Research Letters 24, 1583–1586.
Farnetani, C.G., Samuel, H., 2005. Beyond the thermal plume paradigm. Geophysical Research Letters 32. doi:10.1029/2005GL022360.
Fiquet, G., Auzende, A.L., Siebert, J., Corgne, A., Bureau, H., Ozawa, H., Garbarino, G., 2010. Melting of peridotite to 140 gigapascals. Science 329, 1516–1518.
Fukao, Y., 1992. Seismic tomogram of the Earth's mantle — geodynamic implications. Science 258, 625–630.
Gaherty, J.B., Lay, T., 1992. Investigation of laterally heterogeneous shear velocity structure in D″ beneath Eurasia. Journal of Geophysical Research 97, 417–435.
Garnero, E.J., 2004. A new paradigm for Earth's core–mantle boundary. Science 304. doi:10.1126/science.1097849.
Garnero, E.J., Helmberger, D.V., 1995. A very slow basal layer underlying large-scale low-velocity anomalies in the lower mantle beneath the Pacific — evidence from core phases. Physics of the Earth and Planetary Interiors 91, 161–176.
Garnero, E.J., Helmberger, D.V., 1996. Seismic detection of a thin laterally varying boundary layer at the base of the mantle beneath the central Pacific. Geophysical Research Letters 23, 977–980.
Garnero, E.J., McNamara, A.K., 2008. Structure and dynamics of Earth's lower mantle. Science 320, 626–628.
Ghias, S.R., Jarvis, G.T., 2008. Mantle convection models with temperature- and depth-dependent thermal expansivity. Journal of Geophysical Research 113, B08408.
Glatzmaier, G.A., Schubert, G., Bercovici, D., 1990. Chaotic, subduction-like downflows in a spherical model of convection in the Earth's mantle. Nature 347, 274–277.
Goncharov, A.F., Beck, P., Struzhkin, V.V., Haugen, B.D., Jacobsen, S.D., 2009. Thermal conductivity of lower-mantle minerals. Physics of the Earth and Planetary Interiors 174, 24–32.
Goncharov, A.F., Struzhkin, V.V., Montoya, J.A., Kharlamova, S., Kundargi, R., Siebert, J., Badro, J., Antonangeli, D., Ryerson, F.J., Mao, W., 2010. Effect of composition, structure, and spin state on the thermal conductivity of the Earth's lower mantle. Physics of the Earth and Planetary Interiors 180, 148–153.
Gonnermann, H.M., Manga, M., Jellinek, A.M., 2002. Dynamics and longevity of an initially stratified mantle. Geophysical Research Letters 29, 1399 doi:1310.1029/2002GL014851.
Grand, S.P., 2002. Mantle shear-wave tomography and the fate of subducted slabs. Philosophical Transactions of the Royal Society of London 360, 2475–2491.
Grigne, C., Labrosse, S., Tackley, P.J., 2007. Convection under a lid of finite conductivity in wide aspect ratio models: effect of continents on the wavelength of mantle flow. Journal of Geophysical Research 112. doi:10.1029/2006JB004297.
Gubbins, D., 1998. Interpreting the paleomagnetic field. In: Gurnis, M., Wysession, M.E., Knittle, E., Buffett, B.A. (Eds.), The core–mantle boundary region. American Geophysical Union, pp. 167–182.
Gubbins, D., Alfe, D., Masters, G., Price, G.D., Gillan, M., 2004. Gross thermodynamics of two-component core convection. Geophysical Journal International 157, 1407–1414.
Guignot, N., Andrault, D., 2004. Equations of state of Na–K–Al host phases and implications for MORB density in the lower mantle. Physics of the Earth and Planetary Interiors 143–144, 107–128.
Gurnis, M., 1988. Large-scale mantle convection and the aggregation and dispersal of supercontinents. Nature 332, 695–699.
Gurnis, M., Davies, G.F., 1986. The effect of depth-dependent viscosity on convective mixing in the mantle and the possible survival of primitive mantle. Geophysical Research Letters 13, 541–544.
Hansen, U., Yuen, D.A., 1988. Numerical simulations of thermal-chemical instabilities at the core mantle boundary. Nature 334, 237–240.
Hansen, U., Yuen, D.A., 1989. Dynamical influences from thermal-chemical instabilities at the core–mantle boundary. Geophysical Research Letters 16, 629–632.
Hansen, U., Yuen, D.A., 1994. Effects of depth-dependent thermal expansivity on the interaction of thermal–chemical plumes with a compositional boundary. Physics of the Earth and Planetary Interiors 86, 205–221.
Hansen, U., Yuen, D.A., Kroening, S.E., 1991. Effects of depth-dependent thermal expansivity on mantle circulations and lateral thermal anomalies. Geophysical Research Letters 18, 1261–1264.
Hansen, U., Yuen, D.A., Kroening, S.E., Larsen, T.B., 1993. Dynamic consequences of depth-dependent thermal expansivity and viscosity on mantle circulations and thermal structure. Physics of the Earth and Planetary Interiors 77, 205–223.
He, Y., Wen, L., 2009. Structural features and shear-velocity structure of the "Pacific Anomaly". Journal of Geophysical Research 114, B02309.
Hernlund, J.W., 2010. On the interaction of the geotherm with a post-perovskite phase transition in the deep mantle. Physics of the Earth and Planetary Interiors 180, 222–234.
Hernlund, J.W., Houser, C., 2008. On the statistical distribution of seismic velocities in Earth's deep mantle. Earth and Planetary Science Letters 265, 423–437.
Hernlund, J.W., Jellinek, A.M., 2010. Dynamics and structure of a stirred partially molten ultralow-velocity zone. Earth and Planetary Science Letters 296, 1–8.
Hernlund, J.W., Labrosse, S., 2007. Geophysically consistent values of the perovskite to postperovskite transition Clapeyron slope. Geophysical Research Letters 34. doi:10.1029/2006GL028961.
Hernlund, J.W., Tackley, P.J., 2007. Some dynamical consequences of partial melting in Earth's deep mantle. Physics of the Earth and Planetary Interiors 162, 149–163.
Hernlund, J.W., Thomas, C., Tackley, P.J., 2005. A doubling of the post-perovskite phase boundary and structure of the Earth's lowermost mantle. Nature 434, 882–886.
Herzberg, C., Asimow, P.D., Arndt, N., Niu, Y., Lesher, C.M., Fitton, J.G., Cheadle, M.J., Saunders, A.D., 2007. Temperatures in ambient mantle and plumes: constraints from basalts, picrites, and komatiites. Geochemistry, Geophysics, Geosystems 8, Q02006 doi:02010.01029/02006gc001390.
Hirose, K., 2007. Discovery of post-perovskite phase transition and the nature of D″ layer. In: Hirose, K., Brodholt, J., Lay, T., Yuen, D.A. (Eds.), Post-Perovskite: The Last Mantle Phase Transition, Geophysical Monograph Series 174. American Geophysical Union, pp. 19–35.
Hirose, K., Takafuji, N., Sata, N., Ohishi, Y., 2005. Phase transition and density of subducted MORB crust in the lower mantle. Earth and Planetary Science Letters 237, 239–251.
Hofmann, A.W., 1997. Mantle geochemistry: the message from oceanic volcanism. Nature 385, 219–229.
Hofmeister, A.M., 1999. Mantle values of thermal conductivity and the geotherm from phonon lifetimes. Science 283, 1699–1706.
Hofmeister, A.M., 2008. Inference of high thermal transport in the lower mantle from laser-flash experiments and the damped harmonic oscillator model. Physics of the Earth and Planetary Interiors 170. doi:10.1029/j.pepi.2008.1006.1034.
Honda, S., Yoshida, M., Ootorii, S., Iwase, Y., 2000. The timescales of plume generation caused by continental aggregation. Earth and Planetary Science Letters 176, 31–43.
Houseman, G., 1988. The dependence of convection planform on mode of heating. Nature 332, 346–349.
Huang, J., Davies, G.F., 2007. Stirring in three-dimensional mantle convection models and implications for geochemistry: 2. Heavy tracers. Geochemistry, Geophysics, Geosystems 8, Q07004 doi:07010.01029/02007GC001621.
Hunt, S.A., Weidner, D.J., Li, L., Wang, L., Walte, N.P., Brodholt, J.P., Dobson, D.P., 2009. Weakening of calcium iridate during its transformation from perovskite to post-perovskite. Nature Geoscience 2, 794–797.
Hustoft, J., Catalli, K., Shim, S.-H., Kubo, A., Prakapenka, V.B., Kunz, M., 2008. Equation of state of NaMgF3 postperovskite: implication for the seismic velocity changes in the D″ region. Geophysical Research Letters 35, L10309 doi:10310.11029/12008gl034042.
Hutko, A.R., Lay, T., Revenaugh, J., Garnero, E.J., 2008. Anticorrelated seismic velocity anomalies from post-perovskite in the lowermost mantle. Science 320, 1070–1074.
Ishii, M., Tromp, J., 1999. Normal-mode and free-air gravity constraints on lateral variations in velocity and density of Earth's mantle. Science 285, 1231–1235.
Ito, E., Takahashi, E., 1989. Postspinel transformations in the system Mg_2SiO_4–Fe_2SiO_4 and some geophysical implications. Journal of Geophysical Research 94, 10637–10646.
Jellinek, A.M., Manga, M., 2002. The influence of a chemical boundary layer on the fixity and lifetime of mantle plumes. Nature 418, 760–763.
Kanda, R.V.S., Stevenson, D.J., 2006. Suction mechanism for iron entrainment into the lower mantle. Geophysical Research Letters 33. doi:10.1029/2005GL025009.
Karato, S.-i., 2010. The influence of anisotropic diffusion on the high-temperature creep of a polycrystalline aggregate. Physics of the Earth and Planetary Interiors 183, 468–472.
Karato, S., Karki, B.B., 2001. Origin of lateral variation of seismic wave velocities and density in the deep mantle. Journal of Geophysical Research 106, 21771–21783.
Karato, S., Riedel, M.R., Yuen, D.A., 2001. Rheological structure and deformation of subducted slabs in the mantle transition zone: implications for mantle circulation and deep earthquakes. Physics of the Earth and Planetary Interiors 127, 83–108.
Katsura, T., Yokoshi, S., Kawabe, K., Shatskiy, A., Geeth, M.A., Manthilake, M., Zhai, S., Fukui, H., Chamathni, H.A., Hegoda, I., Yoshino, T., Yamazaki, D., Matsuzaki, T., Yoneda, A., Ito, E., Sugita, M., Tomioka, N., Hagiya, K., Nozawa, A., Funakoshi, K., 2009. P–V–T relations of $MgSiO_3$ perovskite determined by in situ X-ray diffraction using a large-volume high-pressure apparatus. Geophysical Research Letters 36. doi:10.1029/2008GL035658.
Katsura, T., Yoneda, A., Yamazaki, D., Yoshino, T., Ito, E., 2010. Adiabatic temperature profile in the mantle. Physics of the Earth and Planetary Interiors 183, 212–218.
Kawai, K., Geller, R.J., 2010. Waveform inversion for localized seismic structure and an application to D″ structure beneath the Pacific. Journal of Geophysical Research 115. doi:10.1029/2009JB006503.
Kawai, K., Tsuchiya, T., 2009. Temperature profile in the lowermost mantle from seismological and mineral physics joint modeling. Proceedings of the National Academy of Sciences 106, 22119–22123.
Kawai, K., Geller, R.J., Fuji, N., 2007a. D″ beneath the Arctic from inversion of shear waveforms. Geophysical Research Letters 34. doi:10.1029/2007GL031517.
Kawai, K., Takeuchi, N., Geller, R.J., Fuji, N., 2007b. Possible evidence for a double crossing phase transition in D″ beneath central America from inversion of seismic waveforms. Geophysical Research Letters 34. doi:10.1029/2007GL029642.

Kawai, K., Sekine, S., Fuji, N., Geller, R.J., 2009. Waveform inversion for D″ structure beneath northern Asia using Hi-net tiltmeter data. Geophysical Research Letters 36. doi:10.1029/2009GL039651.
Ke, Y., Solomatov, V.S., 2004. Plume formation in strongly temperature-dependent viscosity fluids over a very hot surface. The Physics of Fluids 16, 1059–1063.
Kellogg, L.H., Turcotte, D.L., 1986. Homogenization of the mantle by convective mixing and diffusion. Earth and Planetary Science Letters 81, 371–378.
Kellogg, L.H., Hager, B.H., van der Hilst, R.D., 1999. Compositional stratification in the deep mantle. Science 283, 1881–1884.
Kennett, B.L.N., Gorbatov, A., 2004. Seismic heterogeneity in the mantle — strong shear wave signature of slabs from joint tomography. Physics of the Earth and Planetary Interiors 146, 87–100.
Kesson, S.E., Gerald, J.D.F., Shelley, J.M., 1998. Mineralogy and dynamics of a pyrolite lower mantle. Nature 393, 252–255.
Khan, A., Connolly, J.A.D., Taylor, S.R., 2008. Inversion of seismic and geodetic data for the major element chemistry and temperature of the Earth's mantle. Journal of Geophysical Research 113, B09308 doi:09310.01029/02007jb005239.
King, S.D., 1995. Radial models of mantle viscosity — results from a genetic algorithm. Geophysical Journal International 122, 725–734.
Knittle, E., Jeanloz, R., 1991. Earths core–mantle boundary — results of experiments at high-pressures and temperatures. Science 251, 1438–1443.
Komabayashi, T., Maruyama, S., Rino, S., 2009. A speculation on the structure of the D″ layer: the growth of anti-crust at the core–mantle boundary through the subduction history of the Earth. Gondwana Research 15, 342–353.
Kombayashi, T., Hirose, K., Sugimura, E., Sata, N., Dubrovinsky, L.S., 2008. Simultaneous volume measurements of post-peroskite and perovskite and their thermal equations of state. Earth and Planetary Science Letters 265, 515–524.
Konishi, K., Kawai, K., Geller, R.J., Fuji, N., 2009. MORB in the lowermost mantle beneath the western Pacific: evidence from waveform inversion. Earth and Planetary Science Letters 278, 219–225.
Korenaga, J., 2005. Firm mantle plumes and the nature of the core–mantle boundary region. Earth and Planetary Science Letters 232, 29–37.
Kyvalova, H., Cadek, O., Yuen, D.A., 1995. Correlation analysis between subduction in the last 180 Myr and lateral seismic structure of the lower mantle: geodynamical implications. Geophysical Research Letters 22, 1281–1284.
Labrosse, S., 2002. Hotspots, mantle plumes and core heat loss. Earth and Planetary Science Letters 199, 147–156.
Labrosse, S., Hernlund, J.W., Coltice, N., 2007. A crystallising dense magma ocean at the base of Earth's mantle. Nature 450, 866–869.
Lassak, T.M., McNamara, A.K., Zhong, S., 2007. Influence of thermochemical piles on topography at Earth's core–mantle boundary. Earth and Planetary Science Letters 261, 443–455.
Lassak, T.M., McNamara, A.K., Garnero, E.J., Zhong, S., 2010. Core–mantle boundary topography as a possible constraint on lower mantle chemistry and dynamics. Earth and Planetary Science Letters 289, 232–241.
Lay, T., Garnero, E.J., 2007. Reconciling the post-perovskite phase with seismological observations of lowermost mantle structure. In: Hirose, K., Brodholt, J., Lay, T., Yuen, D.A. (Eds.), Post-Perovskite: The Last Mantle Phase Transition, Geophysical Monograph Series 174. American Geophysical Union, pp. 129–153.
Lay, T., Garnero, E.J., 2011. Deep mantle seismic modeling and imaging. Annual Review of Earth and Planetary Sciences 39, 91–123.
Lay, T., Helmberger, D.V., 1983. A shear velocity discontinuity in the lower mantle. Geophysical Research Letters 10, 63–66.
Lay, T., Hernlund, J., Garnero, E.J., Thorne, M.S., 2006. A post-perovskite lens and D″ heat flux beneath the central Pacific. Science 314, 1272–1276.
Lay, T., Hernlund, J., Buffett, B.A., 2008. Core–mantle boundary heat flow. Nature Geoscience 1, 25–32.
Le Bars, M., Davaille, A., 2002. Stability of thermal convection in two superimposed miscible viscous fluids. Journal of Fluid Mechanics 471, 339–363.
Le Bars, M., Davaille, A., 2004a. Large interface deformation in two-layer thermal convection of miscible viscous fluids. Journal of Fluid Mechanics 499, 75–110.
Le Bars, M., Davaille, A., 2004b. Whole layer convection in a heterogeneous planetary mantle. Journal of Geophysical Research 109, B03403 doi:03410.01029/02003JB002617.
Lee, C.-T., Luffi, P., Hoink, T., Li, J., Dasgupta, R., Hernlund, J., 2010. Upside-down differentiation and generation of a 'primordial' lower mantle. Nature 463, 930–933.
Leng, W., Zhong, S., 2008. Controls on plume heat flux and plume excess temperature. Journal of Geophysical Research 113, B04408 doi:04410.01029/02007jb005155.
Lin, S.-C., van Keken, P.E., 2005. Multiple volcanic episodes of flood basalts caused by thermochemical mantle plumes. Nature 436, 250–252.
Lin, S.-C., Van Keken, P.E., 2006a. Dynamics of thermochemical plumes: 1. Plume formation and entrainment of a dense layer. Geochemistry, Geophysics, Geosystems 7. doi:10.1029/2005GC001071.
Lin, S.-C., Van Keken, P.E., 2006b. Dynamics of thermochemical plumes: 2. Complexity of plume structures and its implications for mapping of mantle plumes. Geochemistry, Geophysics, Geosystems 7. doi:10.1029/2005GC001072.
Lowman, J.P., Jarvis, G.T., 1993. Mantle convection flow reversals due to continental collisions. Geophysical Research Letters 20, 2087–2090.
Malamud, B.D., Turcotte, D.L., 1999. How many plumes are there? Earth and Planetary Science Letters 174, 113–124.
Manga, M., 1996. Mixing of heterogeneities in the mantle — effect of viscosity differences. Geophysical Research Letters 23, 403–406.
Manga, M., Jeanloz, R., 1996. Implications of a metal-bearing chemical-boundary layer in D″ for mantle dynamics. Geophysical Research Letters 23, 3091–3094.
Manthilake, M.A.G.M., de Koker, N., Frost, D.J., McCammon, C.A., 2011. Lattice thermal conductivity of lower mantle minerals and heat flux from Earth's core. Proceedings of the National Academy of Sciences (Electronic publication ahead of print October 20, 2011). doi:10.1073/pnas.1110594108.
Mao, W.L., Mao, H.K., Sturhahn, W., Zhao, J., Prakapenka, V., Shu, J., Fei, Y., Hemley, R.J., 2006. Iron-rich postperovskite and the origin of ultralow-velocity zones. Science 312, 564–565.
Maruyama, S., 1994. Plume tectonics. Journal of the Geological Society of Japan 100, 24–49.
Maruyama, S., Santosh, M., Zhao, D., 2007. Superplume, supercontinent, and post-perovskite: mantle dynamics and anti-plate tectonics on the core–mantle boundary. Gondwana Research 11, 7–37.
Masters, G., Laske, G., Bolton, H., Dziewonski, A., 2000. The relative behavior of shear velocity, bulk sound speed, and compressional velocity in the mantle: Implications for chemical and thermal structure. In: Karato, S., Forte, A.M., Liebermann, R.C., Masters, G., Stixrude, L. (Eds.), Geophysical Monograph on Mineral Physics and Seismic Tomography fom the atomic to the global scale. Americal Geophysical Union, pp. 63–87.
Matas, J., Bukowinski, M.S.T., 2007. On the anelastic contribution to the temperature dependence of lower mantle seismic velocities. Earth and Planetary Science Letters 259, 51–65.
Matas, J., Bass, J., Ricard, Y., Mattern, E., Bukowinski, M.S.T., 2007. On the bulk composition of the lower mantle: predictions and limitations from generalized inversion of radial seismic profiles. Geophysical Journal International 170, 764–780.
Matyska, C., Yuen, D.A., 2005. The importance of radiative heat transfer on superplumes in the lower mantle with the new post-perovskite phase change. Earth and Planetary Science Letters 234, 71–81.
Matyska, C., Yuen, D.A., 2006. Lower mantle dynamics with the post-perovskite phase change, radiative thermal conductivity, temperature- and depth-dependent viscosity. Physics of the Earth and Planetary Interiors 154, 196–207.
Matyska, C., Yuen, D., 2007. Lower-mantle material properties and convection models of multiscale plumes. In: Foulger, G.R., Jurdy, D.M. (Eds.), Plates, Plumes, and Planetary Processes, Geological Society of America Special Paper 430. Geological Society of America, pp. 137–163.
Matyska, C., Yuen, D.A., Wentzcovitch, R.M., Cìzkova, H., 2011. The impact of variability in the rheological activation parameters on lower-mantle viscosity stratification and its dynamics. Physics of the Earth and Planetary Interiors 188, 1–8. doi:10.1016/j.pepi.2011.05.012.
McKenzie, D., 1979. Finite deformation during fluid flow. Geophysical Journal of the Royal Astronomical Society 58, 689–715.
McKenzie, D., Bickle, M.J., 1988. The volume and composition of melt generated by extension of the lithosphere. Journal of Petrology 29, 625–679.
McKenzie, D.P., Roberts, J.M., Weiss, N.O., 1974. Convection in the Earth's mantle: towards a numerical simulation. Journal of Fluid Mechanics 62, 465–538.
McNamara, A.K., Zhong, S., 2004a. The influence of thermochemical convection on the fixity of mantle plumes. Earth and Planetary Science Letters 222, 485–500.
McNamara, A.K., Zhong, S., 2004b. Thermochemical structures within a spherical mantle: superplumes or piles? Journal of Geophysical Research 109. doi:10.1029/2003JB00287.
McNamara, A.K., Zhong, S., 2005. Thermochemical piles beneath Africa and the Pacific Ocean. Nature 437, 1136–1139.
McNamara, A.K., Karato, S.I., van Keken, P.E., 2001. Localization of dislocation creep in the lower mantle: implications for the origin of seismic anisotropy. Earth and Planetary Science Letters 191, 85–99.
McNamara, A.K., Garnero, E.J., Rost, S., 2010. Tracking deep mantle reservoirs with ultra-low velocity zones. Earth and Planetary Science Letters 299, 1–9.
Merkel, S., McNamara, A.K., Kubo, A., Speziale, S., Miyagi, L., Meng, Y., Duffy, T.S., Wenk, H.R., 2007. Deformation of (Mg, Fe)SiO3 post-perovskite and D″ anisotropy. Science 316, 1729–1732.
Mitrovica, J.X., Forte, A.M., 2004. A new inference of mantle viscosity based upon joint inversion of convection and glacial isostatic adjustment data. Earth and Planetary Science Letters 225, 177–189.
Mittelstaedt, E., Tackley, P.J., 2005. Plume heat flow is much less than CMB heat flow. Earth and Planetary Science Letters 241, 202–210.
Miyagi, L., Kanitpanyacharoen, W., Kaercher, P., Lee, K.K.M., Wenk, H.-R., 2010. Slip systems in $MgSiO_3$ post-perovskite: implications for D″ anisotropy. Science 329, 1639–1641.
Monnereau, M., Yuen, D.A., 2002. How flat is the lower-mantle temperature gradient? Earth and Planetary Science Letters 202, 171–183.
Monnereau, M., Yuen, D.A., 2007. Topology of the postperovskite phase transition and mantle dynamics. Proceedings of the National Academy of Sciences 104, 9156–9161.
Monnereau, M., Yuen, D.A., 2010. Seismic imaging of the D″ and constraints on the core heat flux. Physics of the Earth and Planetary Interiors 180, 258–270. doi:10.1029/j.pepi.2009.1012.1005.
Montague, N.L., Kellogg, L.H., 2000. Numerical models for a dense layer at the base of the mantle and implications for the geodynamics of D″. Journal of Geophysical Research 105, 11101–11114.
Morgan, W.J., 1971. Convection plumes in the lower mantle. Nature 230, 42–43.
Mosenfelder, J.L., Asimow, P.D., Ahrens, T.J., 2007. Thermodynamic properties of Mg_2SiO_4 liquid at ultra-high pressures from shock measurements to 200 GPa on forsterite and wadsleyite. Journal of Geophysical Research 112, B06208 doi:06210.01029/02006jb004364.
Mosenfelder, J.L., Asimow, P.D., Frost, D.J., Rubie, D.C., Ahrens, T.J., 2009. The $MgSiO_3$ system at high pressure: thermodynamic properties of perovskite, postperovskite, and melt from global inversion of shock and static compression data. Journal of Geophysical Research 114, B01203 doi:01210.01029/02008jb005900.
Moser, J., Yuen, D.A., Larsen, T.B., Matyska, C., 1997. Dynamical influences of depth-dependent properties on mantle upwellings and temporal variations of the moment of inertia. Physics of the Earth and Planetary Interiors 102, 153–170.
Murakami, M., Hirose, K., Kawamura, K., Sata, N., Ohishi, Y., 2004. Post-perovskite phase transition in $MgSiO_3$. Science 304, 855–858.

Nakagawa, T., Tackley, P.J., 2004a. Effects of a perovskite-post perovskite phase change near the core–mantle boundary on compressible mantle convection. Geophysical Research Letters 31, L16611. doi:10.1029/2004GL020648.

Nakagawa, T., Tackley, P.J., 2004b. Effects of thermo-chemical mantle convection on the thermal evolution of the Earth's core. Earth and Planetary Science Letters 220, 107–119.

Nakagawa, T., Tackley, P.J., 2005a. Deep mantle heat flow and thermal evolution of Earth's core in thermo-chemical multiphase models of mantle convection. Geochemistry, Geophysics, Geosystems 6. doi:10.1029/2005GC000967.

Nakagawa, T., Tackley, P.J., 2005b. The interaction between the post-perovskite phase change and a thermo-chemical boundary layer near the core–mantle boundary. Earth and Planetary Science Letters 238, 204–216.

Nakagawa, T., Tackley, P.J., 2006. Three-dimensional structures and dynamics in the deep mantle: effects of post-perovskite phase change and deep mantle layering. Geophysical Research Letters 33. doi:10.1029/2006GL025719.

Nakagawa, T., Tackley, P.J., 2008. Lateral variations in CMB heat flux and deep mantle seismic velocity caused by a thermal-chemical-phase boundary layer in 3D spherical convection. Earth and Planetary Science Letters 271, 348–358.

Nakagawa, T., Tackley, P.J., 2010. Influence of initial CMB temperature and other parameters on the thermal evolution of Earth's core resulting from thermo-chemical spherical mantle convection. Geochemistry, Geophysics, Geosystems 11. doi:10.1029/2010GC003031.

Nakagawa, T., Tackley, P.J., 2011. Effects of low-viscosity post-perovskite on thermo-chemical convection in a 3-D spherical shell. Geophysical Research Letters 38. doi:10.1029/2010GL046494.

Nakagawa, T., Tackley, P.J., Deschamps, F., Connolly, J.A.D., 2009. Incorporating self-consistently calculated mineral physics into thermo-chemical mantle convection simulations in a 3D spherical shell and its influence on seismic anomalies in Earth's mantle. Geochemistry, Geophysics, Geosystems 10. doi:10.1029/2008GC002280.

Nakagawa, T., Tackley, P.J., Deschamps, F., Connolly, J.A.D., 2010. The influence of MORB and harzburgite composition on thermo-chemical mantle convection in a 3-D spherical shell with self-consistently calculated mineral physics. Earth and Planetary Science Letters 296, 403–412.

Namiki, A., 2003. Can the mantle entrain D″? Journal of Geophysical Research 108. doi:10.1029/2002JB002315.

Ni, S., Tan, E., Gurnis, M., Helmberger, D.V., 2002. Sharp sides to the African superplume. Science 296, 1850–1852.

Ni, S.V., Helmberger, D., Tromp, J., 2005. Three-dimensional structure of the African superplume from waveform modelling. Geophysical Journal International 161, 283–294.

Nimmo, F., Price, G.D., Brodholt, J., Gubbins, D., 2004. The influence of potassium on core and geodynamo evolution. Geophysical Journal International 156, 363–376.

Nomura, R., Ozawa, H., Tateno, S., Hirose, K., Hernlund, J., Muto, S., Ishii, H., Hiraoka, N., 2011. Spin crossover and iron-rich silicate melt in the Earth's deep mantle. Nature 473, 199–202.

Oganov, A.R., Ono, S., 2004. Theoretical and experimental evidence for a post-perovskite phase of $MgSiO_3$ in Earth's D″ layer. Nature 430, 445–448.

Ogawa, M., 2003. Chemical stratification in a two-dimensional convecting mantle with magmatism and moving plates. Journal of Geophysical Research 108. doi:10.1029/2002JB002205.

Ohta, K., 2010. Electrical and thermal conductivity of the Earth's lower mantle, Ph.D. Thesis. Department of Earth and Planetary Sciences, Tokyo Institute of Technology, Tokyo, 276 pp.

Ohta, K., Hirose, K., Lay, T., Sata, N., Ohishi, Y., 2008a. Phase transitions in pyrolite and MORB at lowermost mantle conditions: implications for a MORB-rich pile above the core–mantle boundary. Earth and Planetary Science Letters 267, 107–117.

Ohta, K., Oneda, S., Hirose, K., Sinmyo, R., Shimizu, K., Sata, N., Ohishi, Y., Yasuhara, A., 2008b. The electrical conductivity of post-perovskite in Earth's D″ layer. Science 320, 89–91.

Ohta, K., Hirose, K., Ichiki, M., Shimizu, K., Sata, N., Ohishi, Y., 2010. Electrical conductivities of pyrolitic mantle and MORB materials up to the lowermost mantle conditions. Earth and Planetary Science Letters 289, 497–502.

Ohtani, E., Maeda, M., 2001. Density of basaltic melt at high pressure and stability of the melt at the base of the lower mantle. Earth and Planetary Science Letters 193, 69–75.

Oldham, D., Davies, J.H., 2004. Numerical investigation of layered convection in a three-dimensional shell with application to planetary mantles. Geochemistry, Geophysics, Geosystems 5. doi:10.1029/2003GC000603.

Olson, P., Christensen, U.R., 2002. The time-averaged magnetic field in numerical dynamos with non-uniform boundary heat flow. Geophysical Journal International 151 (3), 809–823.

Olson, P., Kincaid, C., 1991. Experiments on the interaction of thermal convection and compositional layering at the base of the mantle. Journal of Geophysical Research 96, 4347–4354.

Ono, S., Ito, E., Katsura, T., 2001. Mineralogy of subducted basaltic crust (MORB) from 25 to 37 GPa, and chemical heterogeneity of the lower mantle. Earth and Planetary Science Letters 190, 57–63.

Osako, M., Ito, E., 1991. Thermal diffusivity of $MgSiO_3$ perovskite. Geophysical Research Letters 18, 239–242.

Parmentier, E.M., Sotin, C., Travis, B.J., 1994. Turbulent 3-D thermal convection in an infinite Prandtl number, volumetrically heated fluid — implications for mantle dynamics. Geophysical Journal International 116, 241–251.

Peltier, W.R., 1996. Mantle viscosity and ice-age ice-sheet topography. Science 273, 1359–1364.

Peltier, W.R., Drummond, R., 2010. Deepest mantle viscosity: constraints from Earth rotation anomalies. Geophysical Research Letters 37, L12304 doi:12310.11029/12010gl043219.

Peltier, W.R., Jiang, X., 1996. Mantle viscosity from the simultaneous inversion of multiple data sets pertaining to postglacial rebound. Geophysical Research Letters 23, 503–506.

Petford, N., Yuen, D., Rushmer, T., Brodholt, J., Stackhouse, S., 2005. Shear-induced material transfer across the core–mantle boundary aided by the post-perovskite phase transition. Earth Planets Space 57, 459–464.

Petford, N., Rushmer, T., Yuen, D.A., 2007. Deformation-induced mechanical instabilities at the core–mantle boundary. In: Hirose, K., Brodholt, J., Lay, T., Yuen, D.A. (Eds.), Post-Perovskite: The Last Mantle Phase Transition, Geophysical Monograph Series 174. American Geophysical Union, pp. 271–287.

Phipps Morgan, J., 1998. Thermal and rare gas evolution of the mantle. Chemical Geology 145, 431–445.

Poirier, J.P., 1993. Core-infiltrated mantle and the nature of the D″ layer. Journal of Geomagnetism and Geoelectricity 45, 1221–1227.

Poirier, J.P., Le Mouel, J.L., 1992. Does infiltration of core material into the lower mantle affect the observed geomagnetic field? Physics of the Earth and Planetary Interiors 73, 29–37.

Price, G.D., Alfe, D., Vocadlo, L., Gillan, M.J., 2004. The Earth's core: an approach from first principles. In: Sparks, R.S.J., Hawkesworth, C.J. (Eds.), The State of the Planet: Frontiers and Challenges in Geophysics, Geophysical Monograph Series. Amer. Geophys. Union.

Rayleigh, L., 1916. On convective currents in a horizontal layer of fluid, when the higher temperature is on the under side. Philosophical Magazine, Series VI 32, 529–546.

Reuteler, D.M., Yuen, D.A., Balachandar, S., Honda, S., 1993. Three-dimensional mantle convection: effects of depth-dependent properties and multiple phase transitions. International Video Journal of Engineering Research 3, 47–63.

Revenaugh, J., Meyer, R., 1997. Seismic evidence of partial melt within a possibly ubiquitous low-velocity layer at the base of the mantle. Science 277, 670–673.

Ricard, Y., Richards, M., Lithgow-Bertelloni, C., LeStunff, Y., 1993. A geodynamic model of mantle density heterogeneity. Journal of Geophysical Research 98, 21895–21909.

Richards, M.A., Engebretson, D.C., 1992. Large-scale mantle convection and the history of subduction. Nature 355, 437–440.

Richards, M.A., Duncan, R.A., Courtillot, V.E., 1989. Flood basalts and hot-spot tracks — plume heads and tails. Science 246, 103–107.

Richter, F.M., Johnson, C.E., 1974. Stability of a chemically layered mantle. Journal of Geophysical Research 79, 1635–1639.

Richter, F.M., McKenzie, D., 1981. On some consequences and possible causes of layered mantle convection. Journal of Geophysical Research 86, 6133–6142.

Ricolleau, A., Fei, Y., Cottrell, E., Watson, H., Deng, L., Zhang, L., Fiquet, G., Auzende, A.-L., Roskosz, M., Morard, G., Prakapenka, V., 2009. Density profile of pyrolite under the lower mantle conditions. Geophysical Research Letters 36, L06302 doi:06310.01029/02008gl036759.

Ricolleau, A., Perrillat, J.-P., Fiquet, G., Daniel, I., Matas, J., Addad, A., Menguy, N., Cardon, H., Mezouar, M., Guignot, N., 2010. Phase relations and equation of state of a natural MORB: implications for the density profile of subducted oceanic crust in the Earth's lower mantle. Journal of Geophysical Research 115, B08202 doi:08210.01029/02009jb006709.

Ringwood, A.E., 1990. Slab-mantleinteractions.3. Petrogenesis of intraplate magmas and structure of the upper mantle. Chemical Geology 82, 187–207.

Ritsema, J., Van Heijst, H.-J., 2002. Constraints on the correlation of P- and S-wave velocity heterogeneity in the mantle from P, PP, PPP and PKPab traveltimes. Geophysical Journal International 149, 482–489.

Ritsema, J., Heijst, H.J.v., Woodhouse, J.H., 1999. Complex shear wave velocity structure imaged beneath Africa and Iceland. Science 286, 1925–1928.

Ritsema, J., van Heijst, H.J., Woodhouse, J.H., 2004. Global transition zone tomography. Journal of Geophysical Research 109, B02302 doi:02310.01029/02003jb002610.

Robertson, G.S., Woodhouse, J.H., 1996. Ratio of relative S to P velocity heterogeneity in the lower mantle. Journal of Geophysical Research 101, 20041–20052.

Rost, S., Garnero, E.J., Stefan, W., 2010a. Thin and intermittent ultralow-velocity zones. Journal of Geophysical Research 115, B06312 doi:06310.01029/02009jb006981.

Rost, S., Garnero, E.J., Thorne, M.S., Hutko, A.R., 2010b. On the absence of an ultralow-velocity zone in the North Pacific. Journal of Geophysical Research 115, B04312 doi:04310.01029/02009jb006420.

Saltzer, R.L., van der Hilst, R.D., K·rason, H., 2001. Comparing P and S wave heterogeneity in the mantle. Geophysical Research Letters 28, 1335–1338 doi:06310.01029/02003jb002712.

Saltzer, R.L., Stutzmann, E., van der Hilst, R.D., 2004. Poisson's ratio in the lower mantle beneath Alaska: evidence for compositional heterogeneity. Journal of Geophysical Research 109, B06301.

Sammis, C.G., Smith, J.C., Schubert, G., Yuen, D.A., 1977. Viscosity-depth profile of the Earth's mantle: effects of polymorphic phase transitions. Journal of Geophysical Research 82, 3747–3761.

Schubert, G., Zebib, A., 1980. Thermal convection of an internally heated infinite Prandtl number fluid in a spherical shell. Geophysical and Astrophysical Fluid Dynamics 15, 65–90.

Schubert, G., Masters, G., Olson, P., Tackley, P., 2004. Superplumes or plume clusters? Physics of the Earth & Planetary Interiors 146, 147–162.

Senshu, H., Maruyama, S., Rino, S., Santosh, M., 2009. Role of tonalite–trodhjemite–granite (TTG) crust subduction on the mechanism of supercontinent breakup. Gondwana Research 15, 433–442.

Sharpe, H.N., Peltier, W.R., 1978. Parameterized mantle convection and the Earth's thermal history. Geophysical Research Letters 5, 737–744.

Shim, S.-H., Catalli, K., Hustoft, J., Kubo, A., Prakapenka, V.B., Caldwell, W.A., Kunz, M., 2008. Crystal structure and thermoelastic properties of $(Mg_{0.91}Fe_{0.09})$ postperovskite up to 135 GPa and 2700 K. Proceedings of the National Academy of Sciences 105, 7382–7386.

Sidorin, I., Gurnis, M., Helmberger, D.V., 1999a. Dynamics of a phase change at the base of the mantle consistent with seismological observations. Journal of Geophysical Research 104, 15005–15024.

Sidorin, I., Gurnis, M., Helmberger, D.V., 1999b. Evidence for a ubiquitous seismic discontinuity at the base of the mantle. Science 286, 1326–1331.
Simmons, N.A., Forte, A.M., Boschi, L., Grand, S.P., 2010. GyPSuM: a joint tomographic model of mantle density and seismic wave speeds. Journal of Geophysical Research 115, B12310.
Sleep, N.H., 1988. Gradual entrainment of a chemical layer at the base of the mantle by overlying convection. Geophysical Journal 95, 437–447.
Solomatov, V.S., 2001. Grain size-dependent viscosity convection and the thermal evolution of the Earth. Earth and Planetary Science Letters 191, 203–212.
Solomatov, V.S., 2007. Magma oceans and primordial mantle differentiation. In: Stevenson, D.J. (Ed.), Treatise on Geophysics. Elsevier B. V., Amsterdam, pp. 91–119.
Solomatov, V.S., Moresi, L.N., 2002. Small-scale convection in the D″ layer. Journal of Geophysical Research 107. doi:10.1029/2000JB000063.
Solomatov, V.S., Reese, C.C., 2008. Grain size variations in the Earth's mantle and evolution of primordial chemical heterogeneities. Journal of Geophysical Research 113. doi:10.1029/2007JB005319.
Solomatov, V.S., Stevenson, D.J., 1993. Suspension in convective layers and style of differentiation of a terrestrial magma ocean. Journal of Geophysical Research 98, 5375–5390.
Solomatov, V.S., El-Khozondar, R., Tikare, V., 2002. Grain size in the lower mantle: constraints from numerical modeling of grain growth in two-phase systems. Physics of the Earth and Planetary Interiors 129, 265–282.
Song, X., Ahrens, T.J., 1994. Pressure-temperature range of reactions between liquid-iron in the outer core and mantle silicates. Geophysical Research Letters 21, 153–156.
Stacey, F.D., 1992. Physics of the Earth, Third ed. Brookfield Press, Kenmore, Queensland, Australia.
Stackhouse, S., Brodholt, J.P., 2008. Elastic properties of the post-perovskite phase of Fe2O3 and implications for ultra-low velocity zones. Physics of the Earth and Planetary Interiors 170, 260–266.
Stackhouse, S., Brodholt, J., Wookey, J., Kendall, J.-M., Price, G.D., 2005. The effect of temperature on the seismic anisotropy of the perovskite and post-perovskite polymorphs of $MgSiO_3$. Earth and Planetary Science Letters 230, 1–10.
Stackhouse, S., Brodholt, J., Price, G.D., 2006. Elastic anisotropy of $FeSiO_3$ end-members of the perovskite and post-perovskite phases. Geophysical Research Letters 33. doi:10.1029/2005GL023887.
Stackhouse, S., Stixrude, L., Karki, B.B., 2010. Thermal conductivity of periclase (MgO) from first principles. Physical Review Letters 104. doi:10.1103/PhysRevLett.1104.208501.
Steinberger, B., 2000. Plumes in a convecting mantle: models and observations for individual hotspots. Journal of Geophysical Research 105, 11127–11152.
Steinberger, B., Calderwood, A.R., 2006. Models of large-scale viscous flow in the Earth's mantle with constraints from mineral physics and surface observations. Geophysical Journal International 167, 1461–1481.
Stixrude, L., de Koker, N., Sun, N., Mookherjee, M., Karki, B.B., 2009. Thermodynamics of silicate liquids in the deep Earth. Earth and Planetary Science Letters 278, 226–232.
Stracke, A., Hofmann, A.W., Hart, S., 2005. FOZO, HIMU, and the rest of the mantle zoo. Geochemistry, Geophysics, Geosystems 6. doi:10.1016/2004GC000824.
Su, W.-j., Dziewonski, A.M., 1997. Simultaneous inversion for 3-D variations in shear and bulk velocity in the mantle. Physics of the Earth and Planetary Interiors 100, 135–156.
Sun, D., Helmberger, D., 2008. Lower mantle tomography and phase change mapping. Journal of Geophysical Research 113, B10305.
Tackley, P.J., 1996. Effects of strongly variable viscosity on three-dimensional compressible convection in planetary mantles. Journal of Geophysical Research 101, 3311–3332.
Tackley, P.J., 1998. Three-dimensional simulations of mantle convection with a thermochemical CMB boundary layer: D″? In: Gurnis, M., Wysession, M.E., Knittle, E., Buffett, B.A. (Eds.), The Core–Mantle Boundary Region. American Geophysical Union, pp. 231–253.
Tackley, P.J., 2000. Mantle convection and plate tectonics: towards an integrated physical and chemical theory. Science 288, 2002.
Tackley, P.J., 2002. Strong heterogeneity caused by deep mantle layering. Geochemistry, Geophysics, Geosystems 3. doi:10.1029/2001GC000167.
Tackley, P.J., 2007. Mantle geochemical geodynamics. In: Bercovici, D., Schubert, G. (Eds.), Treatise on Geophysics. : Mantle dynamics, Volume 7. Elsevier, pp. 437–505.
Tackley, P.J., 2011. Living dead slabs in 3-D: the dynamics of compositionally-stratified slabs entering a "slab graveyard" above the core–mantle boundary. Physics of the Earth and Planetary Interiors 188, 150–162. doi:10.1029/j.pepi.2011.04.013.
Tackley, P.J., Nakagawa, T., Hernlund, J.W., 2007. Influence of the post-perovskite transition on thermal and thermo-chemical mantle convection. In: Hirose, K., Brodholt, J., Lay, T., Yuen, D.A. (Eds.), The last mantle phase transition. AGU Geophysical Monograph Series, pp. 229–248.
Tan, E., Gurnis, M., 2005. Metastable superplumes and mantle compressibility. Geophysical Research Letters 32, L20307 doi:20310.21029/22005GL024190.
Tan, E., Gurnis, M., 2007. Compressible thermochemical convection and application to lower mantle structures. Journal of Geophysical Research 112, B06304 doi:06310.01029/02006jb004505.
Tan, E., Gurnis, M., Han, L., 2002. Slabs in the lower mantle and their modulation of plume formation. Geochemistry, Geophysics, Geosystems 3, 1067 doi:1010.1029/2001GC000238.
Tan, E., Leng, W., Zhong, S., Gurnis, M., 2011. On the location of plumes and lateral movement of thermo-chemical structures with high bulk modulus in the 3-D compressible mantle. Geochemistry, Geophysics, Geosystems 12, Q07005. doi:10.1029/2011GC003665.
Tang, X., Dong, J., 2010. Lattice thermo conductivity of MgO at conditions of Earth's interio. Proceedings of the National Academy of Sciences 107, 4539–4543.
Tateno, S., Hirose, K., Sata, N., Ohishi, Y., 2009. Determination of post-perovskite phase transition boundary up to 4400 K and implications for thermal structure in D″ layer. Earth and Planetary Science Letters 277, 130–136.
Thomas, C., Garnero, E.J., Lay, T., 2004a. High-resolution imaging of lowermost mantle structure under the Cocos plate. Journal of Geophysical Research 109. doi:10.1029/2004JB003013.
Thomas, C., Kendall, J.M., Lowman, J., 2004b. Lower-mantle seismic discontinuities and the thermal morphology of subducted slabs. Earth and Planetary Science Letters 225, 105–113.
Thompson, P.F., Tackley, P.J., 1998. Generation of mega-plumes from the core–mantle boundary in a compressible mantle with temperature-dependent viscosity. Geophysical Research Letters 25, 1999–2002.
Thorne, M.S., Grand, S.P., Garnero, E.J., 2004. Geographic correlation between hot spots and deep mantle lateral shear-wave velocity gradients. Physics of the Earth and Planetary Interiors 146, 47–63.
To, A., Romanowicz, B., Capdeville, Y., Takeuchi, N., 2005. 3D effects of sharp boundaries at the borders of the African and Pacific superplumes. Earth and Planetary Science Letters 233, 137–153.
Tolstikhin, I.N., Hofmann, A.W., 2005. Early crust on top of the Earth's core. Physics of the Earth and Planetary Interiors 148, 109–130.
Tolstikhin, I.N., Kramers, J.D., Hofmann, A.W., 2006. A chemical Earth model with whole mantle convection: the importance of a core–mantle boundary layer (D″) and its early formation. Chemical Geology 226, 79–99.
Torsvik, T.H., Smethurst, M.A., Burke, K., Steinberger, B., 2006. Large igneous provinces generated from the margins of the large low-velocity provinces in the deep mantle. Geophysical Journal International 167, 1447–1460. doi:10.1111/j.1365-1246X.2006.03158.x.
Torsvik, T.H., M,ller, R.D., Van der Voo, R., Steinberger, B., Gaina, C., 2008. Global plate motion frames: toward a unified model. Reviews of Geophysics 46, RG3004.
Torsvik, T., Burke, K., Steinberger, B., Webb, S.J., Ashwal, L.D., 2010. Diamonds sampled by plumes from the core–mantle boundary. Nature 466, 352–355.
Tosi, N., Cadek, O., Martinec, Z., 2009a. Subducted slabs and lateral viscosity variations: effects on the long-wavelength geoid. Geophysical Journal International 179, 813–826.
Tosi, N., Cadek, O., Martinec, Z., Yuen, D.A., Kaufmann, G., 2009b. Is the long-wavelength geoid sensitive to the presence of postperovskite above the core–mantle boundary? Geophysical Research Letters 36. doi:10.1029/2008GL036902.
Trampert, J., Deschamps, F., Resovsky, J.S., Yuen, D., 2004. Probabilistic tomography maps significant chemical heterogeneities in the lower mantle. Science 306, 853–856.
Tronnes, R.G., 2010. Structure, mineralogy and dynamics of the lowermost mantle. Mineralogy and Petrology 99, 243–261.
Tsuchiya, T., Tsuchiya, J., Umemoto, K., Wentzcovitch, R.A., 2004a. Phase transition in MgSiO3 perovskite in the earth's lower mantle. Earth and Planetary Science Letters 224, 241–248.
Tsuchiya, T., Tsuchiya, J., Umemoto, K., Wentzcovitch, R.M., 2004b. Phase transition in MgSiO3 perovskite in the earth's lower mantle. Earth and Planetary Science Letters 224, 241–248.
Tsuchiya, J., Tsuchiya, T., Wentzcovitch, R.M., 2005. Vibrational and thermodynamic properties o MgSiO3 postperovskite. Journal of Geophysical Research 110. doi:10.1029/2004JB003409.
Tsuchiya, T., Wentzcovitch, R.M., da Silva, C.R.S., de Gironcoli, S., 2006. Spin transition in magnesiow ustite in Earth's lower mantle. Physical Review Letters 96, 198501.
van den Berg, A.P., De Hoop, M.V., Yuen, D.A., Duchkov, A., van der Hilst, R.D., Jacobs, M.H.G., 2010. Geodynamical modeling and multiscale seismic expression of thermo-chemical heterogeneity and phase transitions in the lowermost mantle. Physics of the Earth and Planetary Interiors 180, 244–257.
Van der Hilst, R.D., Widlyantoro, S., Engdahl, E.R., 1997. Evidence for deep mantle circulation from global tomography. Nature 386, 578–584.
van der Hilst, R.D., de Hoop, M.V., Wang, P., Shim, S.-H., Ma, P., Tenorio, L., 2007. Seismostratigraphy and thermal structure of Earth's core–mantle boundary region. Science 315, 1813–1817.
van der Meer, D.G., Spakman, W., van Hinsbergen, D.J.J., Amaru, M.L., Torsvik, T.H., 2010. Towards absolute plate motions constrained by lower-mantle slab remnants. Nature Geoscience 3, 36–40.
Van der Voo, R., Spakman, W., Bijwaard, H., 1999a. Mesozoic subducted slabs under Siberia. Nature 397, 246–249.
Van der Voo, R., Spakman, W., Bijwaard, H., 1999b. Tethyan subducted slabs under India. Earth and Planetary Science Letters 171, 7–20.
Vidale, J.E., Hedlin, M.A.H., 1998. Evidence for partial melt at the core–mantle boundary north of Tonga from the strong scattering of seismic waves. Nature 391, 682–685.
Walte, N., Heidelbach, F., Miyajima, N., Frost, D., 2007. Texture development and TEM analysis of deformed CaIrO3: implications for the D″ layer at the core–mantle boundary. Geophysical Research Letters 34, L08306 doi:08310.01029/02007gl029407.
Wang, Y., Wen, L., 2004. Mapping the geometry and geographic distribution of a very-low velocity province at the base of the Earth's mantle. Journal of Geophysical Research 109. doi:10.1029/2003JB002674.
Wang, Y., Wen, L., 2007. Geometry and P and S velocity structure of the "African Anomaly". Journal of Geophysical Research 112, B05313 doi:05310.01029/02006jb004483.
Wen, L., Helmberger, D.V., 1998. Ultra-low velocity zones near the core–mantle boundary from broadband PKP precurors. Science 279, 1701–1703.
Wenk, H.-R., Cottaar, S., Tome, C.N., McNamara, A., Romanowicz, B., 2011. Deformation in the lowermost mantle: from polycrystal plasticity to seismic anisotropy. Earth and Planetary Science Letters 306, 33–45.
Wentzcovitch, R.A., Tsuchiya, T., Tsuchiya, J., 2006. $MgSiO_3$ postperovskite at D″ conditions. Proceedings of the National Academy of Sciences 103, 543–546.
Wentzcovitch, R.M., Justo, J.F., Wu, Z., da Silva, C.R.S., Yuen, D.A., Kohlstedt, D., 2009. Anomalous compressibility of ferropericlase throughout the iron spin cross-over. Proceedings of the National Academy of Sciences 106, 8447–8452.

Wicks, J.K., Jackson, J.M., Sturhahn, W., 2010. Very low sound velocities in iron-rich (Mg,Fe)O: implications for the core–mantle boundary region. Geophysical Research Letters 37.
Willbold, M., Stracke, A., 2006. Trace element composition of mantle end-members: implications for recycling of oceanic and upper and lower continental crust. Geochemistry, Geophysics, Geosystems 7. doi:10.1029/2005GC001005.
Williams, Q., Garnero, E.J., 1996. Seismic evidence for partial melt at the base of Earth's mantle. Science 273, 1528–1530.
Williams, Q., Revenaugh, J., Garnero, E., 1998. A correlation between ultra-low basal velocities in the mantle and hot spots. Science 281, 546–549.
Wookey, J., Stackhouse, S., Kendall, J.M., Brodholt, J., Price, G.D., 2005. Efficacy of the post-perovskite phase as an explanation for lowermost-mantle seismic properties. Nature 438, 1004–1007.
Wysession, M.E., Lay, T., Revenaugh, J., Williams, Q., Garnero, E., Jeanloz, R., Kellogg, L.H., 1998. The D″ discontinuity and its implications. In: Gurnis, M., Wysession, M.E., Knittle, E., Buffett, B.A. (Eds.), The Core–Mantle Boundary Region, Geophysical Monograph series. AGU, Washington, D. C, pp. 273–297.
Xie, S., Tackley, P.J., 2004a. Evolution of helium and argon isotopes in a convecting mantle. Physics of the Earth and Planetary Interiors 146, 417–439.
Xie, S., Tackley, P.J., 2004b. Evolution of U–Pb and Sm–Nd systems in numerical models of mantle convection. Journal of Geophysical Research 109, B11204. doi:10.1029/2004JB003176.
Yamazaki, D., Karato, S., 2001. Some mineral physics contraints on the rheology and geothermal structure of Earth's lower mantle. American Mineralogist 86, 385–391.
Yamazaki, D., Yoshino, T., Ohfuji, H., Ando, J., Yoneda, A., 2006. Origin of seismic anisotropy in the D″ layer inferred from shear deformation experiments on post-perovskite phase. Earth and Planetary Science Letters 252, 372–378.
Yamazaki, D., Yoshino, T., Matsuzaki, T., Katsura, T., Yoneda, A., 2009. Texture of (Mg, Fe)SiO3 perovskite and ferro-periclase aggregate: Implications for rheology of the lower mantle. Physics of the Earth and Planetary Interiors 174, 138–144.
Yoshino, T., Yamazaki, D., Ito, E., Katsura, T., 2008. No interconnection of ferro-periclase in post-spinel phase inferred from conductivity measurement. Geophysical Research Letters 35, L22303 doi:22310.21029/22008gl035932.
Young, C.J., Lay, T., 1987. Evidence for a shear velocity discontinuity in the lower mantle beneath India and the Indian ocean. Physics of the Earth and Planetary Interiors 49, 37–53.
Young, C.J., Lay, T., 1990. Multiple phase analysis of the shear velocity structure in the region beneath Alaska. Journal of Geophysical Research 95, 17385–17402.
Yu, Y.G., Wentzcovitch, R.M., Tsuchiya, T., Umemoto, K., Weidner, D.J., 2007. First principles investigation of the postspinel transition in Mg_2SiO_4. Geophysical Research Letters 34, L10306 doi:10310.11029/12007gl029462.
Yuen, D.A., Spera, F.J., Hansen, U., Yuen, D.A., Kroening, S.E., 1991. Effects of depth-dependent thermal expansivity on mantle circulations and lateral thermal anomalies. Physical Review B 44, 2108–2121.
Yuen, D.A., Hansen, U., Zhao, W., Vincent, A.P., Malevsky, A.V., 1993. Hard turbulent thermal-convection and thermal evolution of the mantle. Journal of Geophysical Research 98, 5355–5373.
Yuen, D.A., Matyska, C., Cadek, O., Kameyama, M., 2007. The dynamical influences from physical properties in the lower mantle and post-perovskite phase transition. In: Hirose, K., Brodholt, J., Lay, T., Yuen, D.A. (Eds.), The last mantle phase transition. AGU Geophysical Monograph Series, pp. 249–270.
Zerr, A., Diegeler, A., Boehler, R., 1998. Solidus of Earth's deep mantle. Science 281, 243–246.
Zhao, D., 2009. Multiscale seismic tomography and mantle dynamics. Gondwana Research 15, 297–323.
Zhong, S.J., Hager, B.H., 2003. Entrainment of a dense layer by thermal plumes. Geophysical Journal International 154, 666–676.